# EXTRANUCLEAR DNA IN *GREGARINA NIPHANDRODES*

By

MARC A. TOSO

A dissertation submitted in partial fulfillment of
the requirements for the degree of

DOCTOR OF PHILOSOPHY
In Zoology

WASHINGTON STATE UNIVERSITY
School of Biological Sciences

Decemberr 2006

EXTRANUCLEAR DNA IN *GREGARINA NIPHANDRODES*

Abstract

By Marc A. Toso, Ph. D.
Washington State University
December 2006

Chair: Charlotte K. Omoto

Most apicomplexans, including *Plasmodium*, *Toxoplasma*, and *Eimeria*, possess both plastids and corresponding plastid genomes. *Cryptosporidium* lacks both the organelle and the genome. To investigate the evolutionary history of plastids in the Apicomplexa, we tried to determine whether gregarines possess a plastid and/or its genome. We used PCR and Dot-blot hybridization to determine whether the gregarine *Gregarina niphandrodes* possesses a plastid genome. We used an inhibitor of plastid function for any reduction in gregarine infection, and transmission electron microscopy to search for plastid ultrastructure. Despite an extensive search, an organelle of the appropriate ultrastructure in transmission electron microscopy, was not observed. Triclosan, an inhibitor of the plastid-specific enoyl-acyl carrier reductase enzyme, did not reduce host infection by *G. niphandrodes*. Plastid-specific primers produced amplicons with the DNA of *Babesia equi, Plasmodium falciparum*, and *Toxoplasma gondii* as templates, but not with *G. niphandrodes* DNA. Plastid-specific DNA probes, which hybridized to *Babesia equi*, failed to hybridize to *G. niphandrodes* DNA. This evidence indicates that *G. niphandrodes* is not likely to possess either a plastid organelle or its genome. This raises the possibility that the plastid was lost in the Apicomplexan following the divergence of gregarines and *Cryptosporidium*.

Table of Contents

LIST OF TABLES

LIST OF FIGURES

## General Introduction

All mitochondria and plastids were ultimately derived from primary symbiotic events, when eukaryotic ancestors engulfed prokaryotic organisms (Gray, 1992). Mitochondria, believed to be the result of primary endosymbiosis of a proteobacterium (Andersson et al., 2003), are found extensively throughout Eukaryota. Engulfment of cyanobacteria by eukaryotic ancestors was the primary symbiotic event that gave rise to all plastids (McFadden and van Dooren, 2004). Numerous secondary endosymbiotic events followed in which eukaryotes engulfed eukaryotes containing plastids and hence gained plastids (Moreira et al., 2000). These secondary endosymbiotic events spread plastids throughout diverse groups of eukaryotes (Cavalier-Smith, 2000).

Extranuclear DNA has typically been found in mitochondria and plastids. Many genes are transferred from the symbiont's genome to the nuclear genome of the host cell (Bachvaroff et al., 2004). However, varying amounts of DNA remain in the organelle. The remnant DNA in the organelle and the genes transferred to the nucleus are useful tools to reveal evolutionary histories of the organelles and the organisms that harbor them (Kohler et al., 1997); (Zhang et al., 2000); (Fast et al., 2001); (Obornik et al., 2002). These tools can also provide ways to determine whether the absence of an organelle in a particular lineage is due to loss in that lineage or multiple acquisitions of the organelle. (Abrahamsen et al., 2004).

The genomes of Apicomplexan plastids and mitochondria are highly reduced or even totally lost. The Apicomplexan plastid genome is among the smallest plastid genomes known. Most plastid genomes range from 100kb to 200kb, while apicomplexan

genomes are only 35-40kb. Mitochondria genomes from organisms other than apicomplexans range from 16kb to 600kb, while the Apicomplexa mitochondrial genome is extremely small at 6kb and is absent in *Cryptosporidium*. A pattern of small genomes is present in this phylum, sequences have been transferred from the organelles to the nucleus and many sequences appear to have been totally lost. Over time, these genomes are shrinking and perhaps eventually result in the loss of the organelles.

A non-photosynthetic plastid is found in a number of apicomplexans (Lang-Unnasch et al., 1998). Among apicomplexans in which plastids were sought, only *Cryptosporidium* was shown to lack a plastid (Abrahamsen et al., 2004). Mitochondria are found across the phylum; yet *Cryptosporidium,* while retaining a "mitochondrial" organelle, lacks a mitochondrial genome (Abrahamsen et al., 2004). A number of phylogenetic analyses have placed the gregarines as a sister group to *Cryptosporidium* (Carreno et al., 1999; Leander and Ramey, 2006). This close relationship of gregarines to a unique Apicomplexan group that lacks both mitochondrial and plastid genomes makes gregarines a key taxa for studies of plastid and mitochondrial genome evolution.

*G. niphandrodes* Life Cycle (Fig. 1).

Gregarines are unicellular protozoan parasites of invertebrates within the phylum Apicomplexa. The gregarine, *Gregarina niphandrodes* is easily maintained in the laboratory through care of its hose *Tenebrio molitor*, the yellow mealworm beetle. *G. niphandrodes* lifecycle begins with the consumption of a haploid sporozoite by the host (10). The sporozoite in the host intestine grows into a large oblong extracellular trophozoite of ~0.5 _m in length (1). A septum divides the trophozoite into two compartments: a smaller head-like compartment called the protomerite and a large body-

like compartment called the deutomerite. The sexual stage of the life cycle begins with syzygy when two trophozoites join together; the top protomerite of one connects with the base of the other trophozoite's deutomerite (2). Next, the two trophozoites lose their oblong shape, become spherical and produce a hard cyst wall (3). At this point they are called gamonts. The two gamonts encased in a tough cell walls and become gametocysts which are shed with the host frass into the external environment.

Here each nucleus goes through numerous mitotic divisions (4). Male and female gametes develop from each respective gamont (5). The flagellated male gametes fertilize the female gametes (6). The two nuclei from each gamete fuse and form diploid zygotes (7). This, the only diploid stage in the lifecycle, spans a relatively short proportion of the life cycle. A spore wall is formed and the nucleus goes through meiosis I and meiosis II, followed by mitosis, which ultimately results in haploid sporozoites (8). Within the gametocyst are hundreds of sporozoites which eventually burst out in a series of chains (9) to wait for a new host to continue the lifecycle (Fig. 2).

Gregarines present many interesting challenges. Until recently there were hardly any DNA sequences of gregarines deposited in databases (Omoto et al., 2004) and few biochemical observations (Heintzelman, 2004). At present it is not possible to grow gregarines outside of their host. The inability to culture gregarines *in vitro* makes one reliant on a sustained degree of host infection in the gathering of material for experiments.

We used the tough gametocyst to collect sufficient amounts of DNA to search for organellar genomes, and the large trophozoites in microscopy studies to search for extranuclear DNA. To search for plastids and a corresponding genome we used PCR,

Southern hybridization analyses, inhibitor studies, and electron microscopy. To search for mitochondria and the mitochondria genome, PCR and Southern hybridization analyses were utilized. To characterize the extranuclear DNA, cloning of restriction fragments, and Southern hybridization analyses were used. The following is divided into three chapters: one, the search for evidence of a plastid and its genome, two highlights the dramatic changes in ultrastructure at the beginning of the sexual stage, and three, the search for mitochondria and its and its genome.

## LITERATURE CITED


Abrahamsen, M., Templeton, T., Enomoto, S., Abrahante, J., Zhu, G., Lancto, C., Deng, M., Liu, C., Widmer, G., Tzipori, S., Buck, G., Xu, P., Bankier, A., Dear, P., Konfortov, B., Spriggs, H., Iyer, L., Anantharaman, V., Aravind, L. and Kapur, V. 2004. Complete genome sequence of the apicomplexan, *Cryptosporidium parvum*. *Science*, **304**: 441-445.

Andersson, S., Karlberg, O., Canback, B. and Kurland, C. 2003. On the origin of mitochondria: a genomics perspective. *Philos. Trans. R. Soc. Lond. B. Biol. Sci.*, **358**: 165-177.

Bachvaroff, T., Concepcion, G., Rogers, C., Herman, E. and Delwiche, C. 2004. Dinoflagellate expressed sequence tag data indicate massive transfer of chloroplast genes to the nuclear genome. *Protist*, **155**: 65-78.

Carreno, R., Martin, D. and Barta, J. 1999. *Cryptosporidium* is more closely related to the gregarines than to coccidia as shown by phylogenetic analysis of apicomplexan parasites inferred using small-subunit ribosomal RNA gene sequences. *Parasitol. Res.*, **85**: 899-904.

Cavalier-Smith, T. 2000. Membrane heredity and early chloroplast evolution. *Trends Plant Sci*, **5**: 174-182.

Fast, N., Kissinger, J., Roos, D. and Keeling, P. 2001. Nuclear-encoded, plastid-targeted genes suggest a single common orgin for apicomplexan and dinoflagellate plastids. *Mol. Biochem. Evol.*, **18**: 418-426.

Gray, M. 1992. The endosymbiont hypothesis revisited. *Int Rev Cytol*, **141**: 233-357.

Heintzelman, M. 2004. Actin and myosin in *Gregarina polymorpha*. *Cell. Motil. Cytoskeleton*, **58**: 83-95.

Kohler, S., Delwiche, C., Denny, P., Tilney, L., Webster, P., Wilson, R., Palmer, J. and Roos, D. 1997. A plastid of probable green algal origin in apicomplexan parasites. *Science*, **275**: 1485-1489.

Lang-Unnasch, N., Reith, M., Munholland, J. and Barta, J. 1998. Plastids are widespread and ancient in parasites of the phylum Apicomplexa. *Internat. J. Parasitol.*, **28**: 1743-1754.

Leander, B. and Ramey, P. 2006. Cellular Identity of a Novel Small Subunit rDNA Sequence Clade of Apicomplexans: Description of the Marine Parasite Rhytidocystis polygordiae n. sp. (Host: Polygordius sp., Polychaeta). *J Eukaryot Microbiol*, **53**: 280-291.

McFadden, G. and van Dooren, G. 2004. Evolution: red algal genome affirms a common origin of all plastids. *Curr Biol*, **14**: R514-516.

Moreira, D., Le Guyader, H. and H, P. 2000. The origin of red algae and the evolution of chloroplasts. *Nature*, **405**: 69-72.

Obornik, M., Van de Peer, Y., Hypsa, V., Frickey, T., Slapeta, J., Meyer, A. and Lukes, J. 2002. Phylogenetic analyses suggest lateral gene transfer from the mitochondrion to the apicoplast. *Gene*, **285**: 109-118.

Omoto, C., Toso, M., Tang, K. and Sibley, L. 2004. Expressed sequence tag (EST) analysis of gregarine gametocyst development. *Int J Paraitol*, **34**: 1261-1271.

Zhang, Z., Green, B. and Cavalier-Smith, T. 2000. Phylogeny of ultra-rapidly evolving dinoflagellate chloroplast genes: a possible common origin for sporozoan and dinoflagellate plastids. *J Mol Evol*, **51**: 26-40.

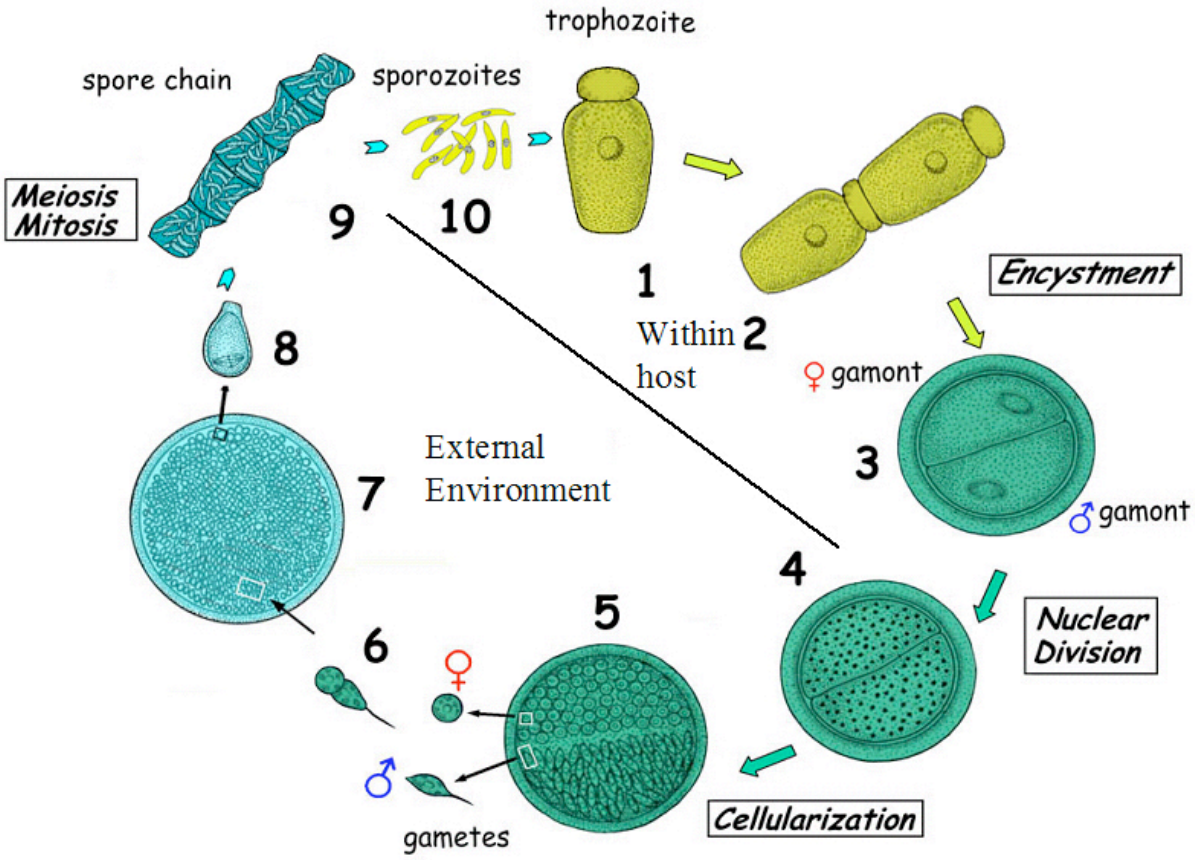


Figure 1. Illustration of *Gregarine niphandrodes* life-cycle.

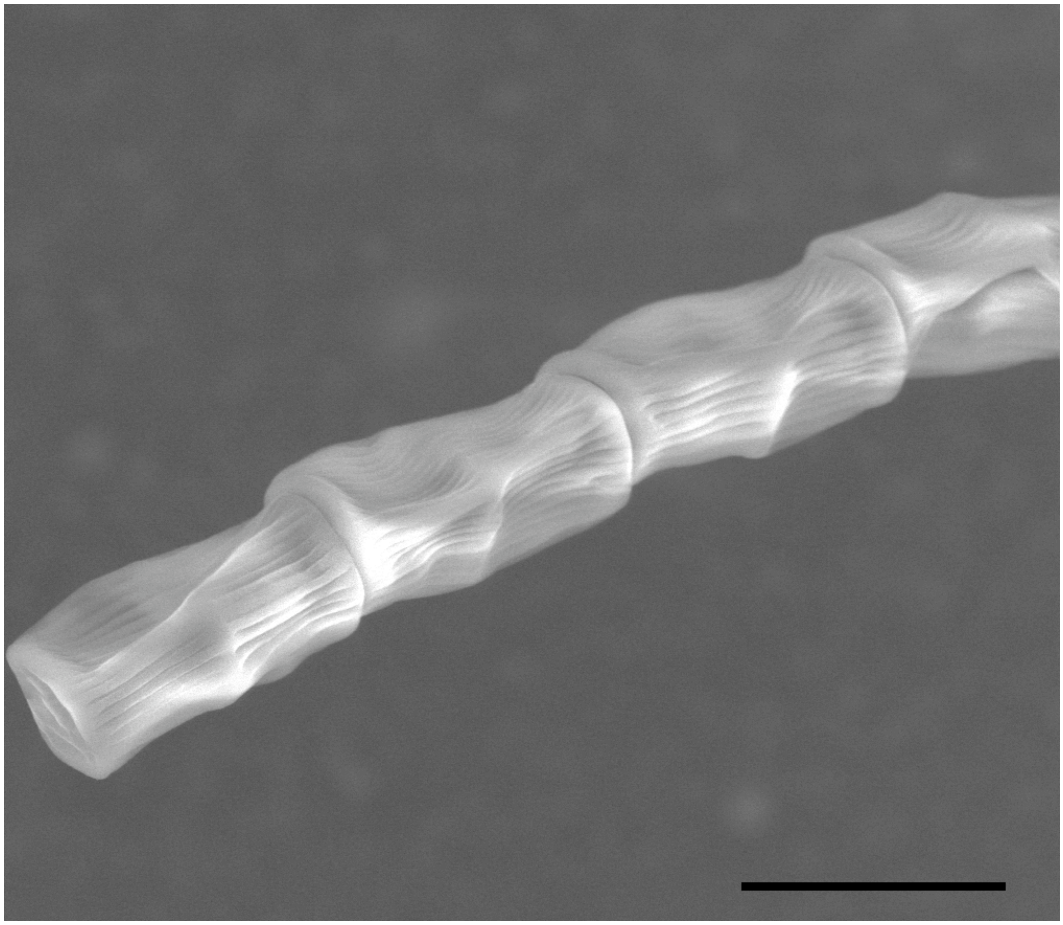

Figure 2. Low vacume SEM image of a *G. niphandrodes* sporozoite chain. Photo by Charlotte Omoto. Scale bar- 5. μm _.

## ATTRIBUTION

Each of the chapters in this dissertation was written in the format required for publication in specified journals. All chapters have been or will be submitted for publication and bear the names of individuals who contributed to their publication. For all manuscripts I was the major contributor and solely responsible for writing each for publications according to journal specifications. Without the assistance of the co-outhors much of the work described in this dissertation would not have been accomplished.

# CHAPTER ONE

## *Gregarina niphandrodes* may lack both a plastid genome and organelle.

**MARC A. TOSO and CHARLOTTE K. OMOTO**

School of Biological Sciences, Washington State University, Pullman, Washington 99164-4236, USA

[Formatted for The Journal of Eukaryotic Microbiology]

Corresponding Author: C.K. Omoto, PO Box 4236,

Washington State University, Pullman, WA 99164-4236

Tel: 509-335-5591; Fax 509-335-3184; Email:omoto@wsu.edu

ABSTRACT

Gregarines are early diverging apicomplexans that appear to be closely related to *Cryptosporidium*. Most apicomplexans, including *Plasmodium*, *Toxoplasma*, and *Eimeria*, possess both plastids and corresponding plastid genomes. *Cryptosporidium* lacks both the organelle and the genome. To investigate the evolutionary history of plastids in the Apicomplexa, we tried to determine whether gregarines possess a plastid and/or its genome. We used PCR and Dot-blot hybridization to determine whether the gregarine *Gregarina niphandrodes* possesses a plastid genome. We used an inhibitor of plastid function for any reduction in gregarine infection, and transmission electron microscopy to search for plastid ultrastructure. Despite an extensive search, an organelle of the appropriate ultrastructure in transmission electron microscopy, was not observed. Triclosan, an inhibitor of the plastid-specific enoyl-acyl carrier reductase enzyme, did not reduce host infection by *G. niphandrodes*. Plastid-specific primers produced amplicons with the DNA of *Babesia equi, Plasmodium falciparum*, and *Toxoplasma gondii* as templates, but not with *G. niphandrodes* DNA. Plastid-specific DNA probes, which hybridized to *Babesia equi*, failed to hybridize to *G. niphandrodes* DNA. This evidence indicates that *G. niphandrodes* is not likely to possess either a plastid organelle or its genome. This raises the possibility that the plastid was lost in the Apicomplexan following the divergence of gregarines and *Cryptosporidium*.

**Key Words.** Apicomplexa, apicoplast, fatty acid synthesis, gregarine

INTRODUCTION

The phylum Apicomplexa consists of unicellular parasites that infect a wide variety of hosts. Apicomplexans that cause diseases in humans or livestock, such as coccidiosis, babesiosis, toxoplasmosis, and malaria, are well studied. Gregarines are apicomplexans that infect invertebrates and have primarily a monoxenous lifecycle. They are considered to represent an early diverging apicomplexan lineage, thus making them a key group for questions regarding apicomplexan evolution. Phylogenetic analyses of the small subunit ribosomal RNA gene suggests the gregarines are a sister group to *Cryptosporidium*, and represent an early divergence within the phylum Apicomplexa (Carreno et al. 1999; Leander et al. 2003). Lifecycle characteristics shared between gregarines and *Cryptosporidium* also suggest that these two groups are sisters (Hijjawi et al. 2002; Rosales et al. 2005).

Apicoplasts are non-photosynthetic plastids found in a number of apicomplexans (Lang-Unnasch et al., 1998). Discovery of the ~35--40 kb plastid genome was a surprise since apicomplexans are non-photosynthetic. However, the presence of plastid DNA indicated that they had a photosynthetic ancestor (Cai et al. 2004; Kohler et al. 1997; McFadden and van Dooren 2004). To date, four species of apicomplexans have had their entire plastid DNA sequenced: *Plasmodium falciparum* (Wilson et al. 1996), *Theileria parva* (Gardner et al. 2005), *Toxoplasma gondii,* and *Eimeria tenella* (Cai et al. 2004). The genes encoded by the small apicoplast genome constitute only a small fraction of the gene products in the apicoplast. Due to the extensive gene transfer from the plastid to the nucleus most of the plastid-localized proteins are encoded in the nuclear DNA (Waller et al. 1998).

*Cryptosporidium* is the only member of the phylum Apicomplexa in which a plastid has been sought but not found. Analysis of the complete genomes of *C. parvum* and *C. hominis* identified neither a plastid genome nor genes with putative plastid-targeting sequences (Abrahamsen et al. 2004; Xu et al. 2004). Primers designed to amplify plastid-encoded sequences failed to produce products with *Cryptosporidium* DNA, yet did produce products using *T. gondii* and *B. bovis* DNA as templates. Likewise, apicomplexan plastid probes failed to hybridize to *C. parvum* DNA, yet hybridized to DNA from *T. gondii*, *P. falciparum*, and *E. bovis* (Zhu et al. 2000a). Plastid-like structures have not been revealed through microscopy of *Cryptosporidium* (Riordan et al. 2003). Cyanobacterial-like genes have been discovered in *Cryptosporidium*; however, they lack plastid-targeting sequences (Huang et al. 2004). Together this evidence indicates that *Cryptosporidium* does not have a plastid genome or the organelle.

A common pathway among plastid bearing organisms is the Type II Fatty Acid Synthesis (FAS II) pathway. This pathway is associated with both plants (Harwood 1996) and apicomplexan plastids (Waller et al. 1998) and is derived from the plastid's ancestral endosymbiont. Inhibitors to this pathway have been shown to stymie *P. falciparum* growth and survival (Surolia and Surolia 2001). *Cryptosporidium* lacks the FAS II pathway and compounds that inhibit this pathway have no effect on *Cryptosporidium* (Zhu et al. 2000b), providing further supporting evidence that *Cryptosporidium* lacks a plastid.

The lack of a plastid in *Cryptosporidium* raises the question of when this organelle was introduced or lost in the apicomplexan lineage. That is, did the lineage leading to

apicomplexans have plastids and subsequently the branch leading to *Cryptosporidium* lose them? Alternatively, did the incorporation of this organelle occur in the apicomplexan lineage after the branch leading to *Cryptosporidium*? Whether gregarines have a plastid is key to answering these questions.

MATERIALS AND METHODS

**Collection of gametocysts from *Gregarina niphandrodes***. Briefly, gametocysts from *G. niphandrodes* were collected from the frass of adult *Tenebrio molitor*, separated on a step sucrose gradient, manually collected, extensively washed in sterile distilled water, and stored in ethanol at –20 °C (Omoto et al., 2004). Gametocysts collected in the triclosan drug study (see below) were not dehydrated in ethanol so that they could be returned to their respective host populations.

**Extraction of DNA from gametocysts of *Gregarina niphandrodes*.** Ethanol-preserved gametocysts from *G. niphandrodes* were hydrated in sterile distilled water. The samples were frozen for 20 min at –80 $^{o}$C and incubated at 50 $^{o}$C for 15 min in lysis buffer (50 mM Tris-HCL, pH 8, 200 mM NaCl, 1 mM EDTA, pH 8, 1% (w/v) SDS, 0.2% (v/v) DTT). DNA was extracted using standard phenol-chloroform-isoamyl extraction and ethanol precipitation. The final pellet was suspended in sterile distilled water.

**PCR**. Six pairs of degenerate plastid-specific primers were used to amplify highly conserved regions of the plastid genome (Table 1) (Zhu et al. 2000a). To account for mismatched bases between template DNA and primers a 5mM magnesium concentration and annealing temperature of 48 $^{o}$C were used. DNA from *B. equi, P. falciparum*, and *T. gondii* was used for plastid positive controls. Primers designed to amplify the nuclear

large subunit rRNA gene from *G. niphandrodes* were used for the positive control for *G. niphandrodes* DNA (Table 1). PCR products were separated by electrophoresis using 1% (w/v) Tris-Acetate-EDTA agarose.

*Babesia equi* products (*, Fig 1) were excised from the gel, re-amplified, and sequenced. DNA sequencing was carried out by the DyeDeoxy terminator cycle protocol with synthetic primers synthesized by Invitrogen (Carlsbad, CA). Sequencing reactions were analyzed on an Applied Biosystems 377 DNA Sequencer at the Washington State University Laboratory of Bioanalysis and Biotechnology.

**Triclosan/bran preparation**. Triclosan (Irgasan™, Sigma-Aldrich, city, state), was dissolved in acetone and applied to wheat bran at 2 concentrations: 4 mg/g of bran and 0.4 mg/g bran. The acetone was allowed to evaporate completely overnight in a fume hood. Control with just acetone was also prepared.

**Beetle care.** Fifty adult beetles (*T. molitor*) from the laboratory stock of beetles infected with *G. niphandrodes* were placed in each concentration of the triclosan/bran mixture. Beetles were tested in triplicate at each concentration of triclosan.

The bran with beetles was covered with an unbleached paper towel. Four ml of water were dropped on the paper towel daily. Every seven days the numbers of beetles were counted and gametocysts were collected from each group as described above and replaced in the container. The bran was replaced every seven days with triclosan-acetone-treated bran for each group's respective treatment. This was continued for forty-two days.

**Thin layer chromatography (TLC)**. To determine the level of triclosan in the intestinal environment of the gregarines, TLC was used. After one week, five beetles each from the 0.4 mg/g and the 4.0 mg/g groups were dissected and the intestines were

frozen at –20 $^{o}$C for 20 min in 1.5-mL microfuge tubes. The tissue was homogenized and the triclosan extracted with a 1:1 (v/v) mixture of methanol:chloroform. An intestine from a beetle in the acetone group was used as a negative control. For a triclosan positive control, an intestine from a beetle unexposed to triclosan was used, but spiked with 1.5 μg of triclosan prior to extraction. The samples were analyzed on Silica Gel 60F254 TLC sheet (EM Separations) with chloroform as solvent and visualized under short wavelength UV illumination.

**Determination of triclosan concentration in beetle intestine.** The intestines of five beetles were placed in a graduated 1.5-ml microfuge tube and centrifuged for one minute at 13000 X *g* to estimate the intestine volume. Five intestines occupied approximately ~100 _l; thus, the average volume of a beetle intestine is ~20 _l. To estimate the quantity of triclosan in the beetle intestine, a triclosan standard from 0.2--1.6 μg TLC was made. This standard was then visually compared with the TLC from each triclosan-exposed beetle. The quantity of triclosan found in the intestines of drugged beetles divided by the intestinal volume provided an estimated concentration of triclosan in the intestines. Our procedure for volume estimate will err on the high end, and thus lower the estimate for the triclosan concentration.

**Determination of gregarine infection.** The level of gregarine infection was assessed by counting gametocysts weekly (see above). As beetles naturally died over time, the ratio of gametocysts per beetle was calculated. The natural log of this ratio was used as the response variable in our analysis. We performed a repeated measures analysis of variance (ANOVA) with time (the 7 time points) and treatment (control/acetone, 4.0

mg/g, 0.4 mg/g) as our factors. The log-transformed response satisfied the assumptions of normality and homogeneity of variances.

At the end of the experimental treatment, five beetles from each group were selected at random for dissection. The dissected intestines were placed in insect Ringer's (120 mM NaCl, 1.2 mM KCl, 1.4 mM $CaCl_2$), and the trophozoites were counted under a dissecting microscope. Trophozoite counts were log-transformed as above and analyzed using a one-way ANOVA to assess the differences between the three treatments.

**Transmission Electron Microscopy**. Trophozoites of *G. niphandrodes* were dissected from *T. molitor* in insect Ringer's solution and fixed overnight at 4 $^{o}$C in 2% (w/v) paraformaldehyde and 2% (v/v) glutaraldehyde in 0.1 M cacodylate buffer, pH 7.2. Samples were rinsed three times in 0.1 M cacodylate buffer prior to a 1-h postfix with 2% (w/v) osmium tetroxide in 0.1 M cacodylate buffer. They were rinsed three times in distilled water and stained in 1% (w/v) tannic acid for 1 h. For potassium permanganate fixation, trophozoites were fixed overnight with 1% (w/v) potassium permanganate in 0.1M veronal acetate buffer. The trophozoites were then washed three times in the buffer. All the specimens were dehydrated in an acetone series and embedded in Spurr's resin. Ultrathin sections were cut with a glass knife on a Leica Reichert microtome and placed on formvar-coated copper grids. Sections were stained with uranyl acetate and Sato's lead. Samples fixed with potassium permanganate were viewed unstained. The samples were viewed on a JEOL 1200 EX TEM. Five trophozoites each from the paraformaldehyde/glutaraldehyde fixation and potassium permanganate fixation were serially sectioned longitudinally. Since trophozoites are large, one section covers a large

proportion of the grid (~300_m x ~125 _m per cell). At least three whole sections were examined from each cell.

**Dot-blot hybridizations.** Hybridizations were performed according to the manufacturer's directions (Boehringer Mannheim DIG System Users Guide). Five-hundred ng of total DNA from *G. niphandrodes* and *B. equi* were denatured by boiling for 10 min, placed on ice, and then dotted onto a Nytran Plus (Florham Park, New Jersey) nylon membrane. The DNA was cross-linked to the membrane using a Bio-Rad GS Gene Linker (Hercules, CA). Probes used were apicoplast PCR products from *B. equi* (PCR products 1, 2, 4, and 5, Fig. 1) and LSU PCR product from *G. niphandrodes* (Lane 7, Fig. 1) labeled with digoxigenin using the PCR DIG Probe Synthesis Kit (Roche Diagnostics, Basel, Switzerland.). Probes were denatured by boiling for 10 min followed by icing. The membrane was pre-hybridized with DIG Easy Hyb buffer (Roche Diagnostics) at 42 °C for 2 h. Hybridization was performed overnight at 42 °C with the DIG-labeled *B. equi* probes in Easy Hyb buffer. After hybridization, the membrane was washed three times in 2.0 _ SSC and 0.1% (w/v) SDS at 50 $^{o}$C. Detection of probe was performed using anti-DIG-AP conjugate (Roche Diagnostics) and the luminescence signal was detected and imaged using an AutoBiochemi (UVP, Upland, CA) system. The membrane was stripped by incubating two times for 20 min in 0.2 M NaOH and 0.1% SDS at 37 $^{o}$C. The membrane was rinsed in 2.0 _ SSC and used again directly for hybridization.

RESULTS

**PCR analysis of DNA from *Gregarina niphandrodes***. PCR was performed to investigate if *G. niphandrodes* possesses DNA sequences similar to those found in other apicomplexan plastids. Six plastid-specific primer pairs designed against highly

conserved regions of the plastid genome (Table. 1) did not produce any products using *G. niphandrodes* DNA as a template despite numerous attempts with different PCR conditions (top row, lanes 1--6, Fig. 1). Products were amplified with primers pairs using *B. equi* DNA as a template (bottom row, lanes 1--6, Fig. 1). The PCR conditions used favored primer hybridization with a slight mismatch in the primer sequence for both *B. equi* and *G. niphandrodes* DNA. The multiple bands observed with *B. equi* DNA as template is attributed to our use of these conditions, since we did not try to optimize the conditions to produce a single amplicon band.

The *B. equi* products (*, Fig. 1) were re-amplified and sequenced to determine whether the products were indeed apicoplast sequences. These sequences had highly significant matches to apicoplast genome sequences: for example, the sequence of the product in lane 4 matched *B. bigemina* apicoplast small subunit ribosomal RNA gene (Accession: AF040968) with an e value of $1e^{-20}$. Thus, the plastid-specific primers amplified plastid sequences of *B. equi* DNA.

We also used primer pairs 1 and 5 with *T. gondii* and *P. falciparum* DNA as templates, and they, too, produced products (data not shown). Yet, no plastid-specific primers amplified products from *G. niphandrodes* DNA. However, primers designed to amplify the conserved nuclear LSU rRNA produced an amplicon with both *G. niphandrodes* and *B. equi* DNA (lane 7, Fig. 1). The sequence of *G. niphandrodes* product from lane 7 (Accession: DQ837379) has a highly significant match to other apicomplexan nuclear LSU rRNA. The *G. niphandrodes* DNA has also been used to amplify and sequence the largest subunit of the DNA-dependent RNA polymerase (RPB1), which is a nuclear protein-encoding gene (Accession: AY168016). Thus, the

quality of *G. niphandrodes* was sufficient for PCR amplification, but it did not produce any product using plastid-specific primers designed for highly conserved apicoplast sequences.

**Triclosan Drug Studies.** Intestines from 5 beetles each from low and high triclosan treatments (0.4 mg/g bran and 4 mg/g bran) and acetone control, and an unexposed beetle but spiked with 1.5 _g of triclosan were extracted and analyzed. Triclosan was not detectable in the intestine of a beetle unexposed to the triclosan (Fig. 2). The beetles exposed to 0.4 mg/g triclosan bran had ~0.3 _g triclosan. The beetles exposed to 4.0 mg/g triclosan bran had ~1.5 _g triclosan. Using ~20 _l as the volume of an intestine, the triclosan concentration is estimated to be ~15,000 ng/ ml at the lower dose of triclosan and ~75,000 ng/ml in the high triclosan treatment.

To determine the effect of triclosan exposure on gregarine infestation of beetles, gametocysts released in the frass of the beetles were counted weekly for 7 weeks. The results indicated no treatment effect ($F=0.15$; $P=0.860$) with no effect of time and no treatment interaction ($F= 0.86$; $P=0.589$).

After the final collection of gametocysts at week 7, five beetles from each group were dissected to determine the degree of trophozoite infection. The huge variance between the numbers of trophozoites between individuals is evident in the large standard deviation for the average number of trophozoites: control (18.4±26.5), 0.4 mg/g (33.3±42.3), and 4.0 mg/g (44.5±56.0). The higher number of trophozoites in both triclosan treatments compared to the control and the higher number of trophozoites in the higher concentration of triclosan was slightly significant ($F=4.53$; $P=0.017$). Thus,

triclosan, a specific inhibitor of FAS II pathway, if anything, increased rather than decreased gregarine infestation.

**Electron Microscopy.** Transmission electron microscopy (TEM) was used to search for plastid-like organelles. Both fixative treatments revealed mitochondrion-like structures (Fig. 3, 5, 6). Despite extensive searches through multiple sections from 10 different trophozoites, no multi-membranous organelle characteristic of plastids was observed. Other membranous organelles, such as epicytic folds and Golgi (Fig. 4) were visible. While potassium permanganate fixation is poor overall, it is useful for revealing membranes, making it an ideal method to reveal multi-membranous organelles, like the plastid. Using this fixation, mitochondria were clearly seen scattered throughout the cytoplasm (Fig. 5). At higher magnification, the details of the mitochondria, their cristae and the dual membranes, are visible (Fig. 6). Various examples of cytoplasm are visible in figure 7, no structures were observed with features reminiscent of plastids in any sections.

**Dot-blot hybridization.** Hybridizations were also used to investigate if *G. niphandrodes* possesses plastid DNA. A mixture of LSU and SSU plastid sequences from *B. equi* plastid DNA (total of ~4 kb) was used to probe for plastid DNA. The hybridizations were performed at a lower stringency to allow for cross species hybridization. The plastid probes hybridized to total DNA from *B. equi*. However, there was no hybridization signal with *G. niphandrodes* DNA (Fig. 8A). The nuclear LSU probe from *G. niphandrodes* hybridized to both the *G. niphandrodes* and *B. equi* DNA (Fig. 8B).

DISCUSSION

We used PCR, an inhibitor specific to a plastid pathway, thin section electron microscopy, and dot-blot hybridization to investigate whether *G. niphandrodes* has a plastid. None of the four approaches provided any evidence to suggest that *G. niphandrodes* possesses a plastid.

No amplicons were obtained with plastid-specific primers using *G. niphandrodes* DNA as a template. This DNA produced amplicons with primers to nuclear LSU and to a nuclear protein-encoding gene, RPB1, clearly demonstrating that the DNA was of sufficient quality to amplify sequences. The plastid-specific primers have been shown to amplify DNA from numerous apicomplexan species, as well as chloroplast DNA (Zhu et al. 2000a), and we produced amplicons using *B. equi*, *T. gondii* and *P. falciparum* templates as positive controls. Thus, if *G. niphandrodes* possesses a plastid genome, our results indicate that its sequence must be significantly divergent from those of other organisms harboring plastids. Obornik et al. (2002) also tried to determine whether the gregarine *Gregarina garnhami* possessed a plastid genome using a plastid-specific SSU rRNA PCR primers but they also could not produce a product.

We investigated whether triclosan reduced the level of *G. niphandrodes* infection in *T. molitor.* We initially tested a range of triclosan concentrations to determine the maximum concentration that did not cause significant beetle mortality over a one week period (data not shown). We then used triclosan at that concentration, 4 mg/g bran, and also at 10-fold lower concentration.

The FASII pathway is found in all organisms harboring plastids (Harwood 1996; Ryall et al. 2003; Waller et al. 1998). Within this pathway, ENR is inhibited by the

compound triclosan in bacteria (Escalada et al. 2005) and in other apicomplexans that contain plastids (McLeod et al. 2001; Surolia and Surolia 2001). *Cryptosporidium* synthesizes fatty acids with a giant multienzymatic Type I FAS (Zhu 2004) and not by the FASII (Abrahamsen et al. 2004; Xu et al. 2004; Zhu et al. 2000a). Consequently, it is unaffected by inhibitors of the FASII pathway (Zhu 2004). If *G. niphandrodes* contained a plastid, we expected triclosan treatment to inhibit the FASII and significantly decrease the number of gametocysts and trophozoites. There was no statistically significant reduction in gametocyst production with triclosan treatment. Unexpectedly, there were HIGHER numbers of trophozoites in the triclosan treatments compared to controls, though it was only slightly statistically significant. Thus, triclosan clearly does NOT decrease the level of gregarine infection in *T. molitor* adults. The higher trophozoite numbers in triclosan-treated beetles and higher trophozoite numbers in the higher triclosan treatment may be explained by triclosan inhibition of the bacterial flora within the intestine. The bacteria may act as competitors to gregarine growth and/or survival. Hence, inhibiting the bacteria with triclosan may indirectly benefit gregarines and lead to higher survival.

Triclosan inhibits ENR through the binding of specific amino acids; bacteria (*E. coli*), plants (*B. napus*), and *P. falciparum* all share identical amino acid sequence at this binding site, indicating a conserved target for triclosan in a wide range of organisms (McLeod et al. 2001). Previous studies on apicomplexans used direct application of triclosan on the parasites to inhibit growth and survival. However, we cannot grow gregarines in the absence of the host. Therefore, we grew the hosts in triclosan to determine its effect upon *G. niphandrodes*. We estimated the concentration of triclosan in

the intestine to be ~15,000 ng/ ml at the lower exposure concentration of triclosan. Previous studies showed that direct exposure of 150 ng/ml for *P. falciparum* and 62 ng/ml for *T. gondii* inhibited their growth (McLeod et al. 2001). Thus, our gregarines were estimated to be exposed to at least 100 times the concentration of triclosan shown to be inhibitory in previous studies.

Triclosan clearly did not decrease gregarine infestation. Indeed, perhaps the increased gregarine infestation strongly indicates that *G. niphandrodes* lacks this common plastid localized enzyme. *Gregarina niphandrodes* may obtain fatty acids from its host, *T. molitor,* making this pathway unessential. However, in that case, it suggests that it may also not require a plastid. This triclosan study is the first to probe the fatty acid metabolism of gregarines, suggesting *G. niphandrodes*, like *Cryptosporidium,* may lack the FASII pathway.

The apicoplast is a multimembranous organelle. Two to 4 membranes have been observed in the Apicomplexa (Hopkins et al. 1999; Kohler et al. 1997; McFadden et al. 1996). The observation of three or four membranes led to the hypothesis that the apicoplast arose through secondary endosymbiosis of an alga. However, studies of the *T. gondii* apicoplast have revealed 2 membranes that undergo complex infoldings, in effect revealing 3--4 membrane layers in thin section. Such a structure suggests an alternative evolutionary pathway for the plastid in *T. gondii* as a primary endosymbiosis of a cyanobacteria (Kohler 2005). We looked for a multimembranous organelle characteristic of plastid ultrastructure in TEM. No organelle with this ultrastructure was observed. Common membranous structures were seen, such as mitochondria and Golgi. The application of permanganate fixation, which is particularly useful for revealing multi-

membrane structures, revealed the dual membrane mitochondria, but also failed to reveal plastid-like organelles.

Dot-blot hybridization also failed to demonstrate a plastid genome in *G. niphandrodes*. The experiment was performed using probes that encompass significant portion of highly conserved plastid sequences at lower stringency to allow for hybridization of mismatched bases between the probe DNA of *B. equi* and *G. niphandrodes*. The apicoplast probe bound to *B. equi* DNA but not to *G. niphandrodes* DNA. This provides further support that *G. niphandrodes* lacks the homologues of SSU and LSU apicoplast sequences. A nuclear LSU *G. niphandrodes* probe was used as a positive control. This hybridization was performed at a low stringency to replicate the conditions of the apicoplast probe hybridizations. The nuclear LSU probe bound to both *G. niphandrodes* and *B. equi* DNA.

Collectively these four studies provide strong evidence that *G. niphandrodes* may not possess either a plastid organelle nor a plastid genome. The shared ancestry of apicomplexan plastids with dinoflagellate plastids implies that the common ancestor of the Apicomplexa, and thus the ancestor of gregarines and *Cryptosporidium* harbored a plastid. Studies of the nuclear-encoded plastid targeted glyceraldehyde-3-phosphate dehydrogenase (GAPDH) gene indicate a common origin of the apicomplexan plastids and the dinoflagellate plastids and its cyanobacterial/algal origin (Fast et al. 2001). Consistent with this hypothesis, analysis of the genome of *C. parvum* revealed several genes of cyanobacterial/algal origin (Huang et al. 2004). The close relationship between gregarines and *Cryptosporidium* within the Apicomplexa and the possible absence of a

plastid in both suggest that the plastid was lost following the divergence of *Cryptosporidium* and gregarines from the other apicomplexan species harboring a plastid.

ACKNOWLEDGMENTS

We thank the WSU Franceschi Microscopy and Imaging Center, namely Chris Davitt, Valerie Lynch-Holm, and the late Vince Franceschi for assistance and guidance in microcopy. Eric Roalson for help and insight. Don Knowles and Lowell Kappmeyer for *B. equis* DNA and technical assistance. Jean Feagin for *T. gondii* and *P. falciparum* DNA and helpful advice. Michelle Martin and Kyle Martin, for gametocysts collection. Derek Pouchnik, WSU Laboratory for Bioanalysis and Biotechnology, for DNA sequencing. Dr. John Janovy, University of Nebraska, Lincoln, for instruction with *T. molitor* and gregarine care. John Dahl and Eric Shelden for technical assistance. Nairanjana Dasgupta, for statistical analysis of the triclosan data.

LITERATURE CITED

Abrahamsen, M., Templeton, T., Enomoto, S., Abrahante, J., Zhu, G., Lancto, C., Deng, M., Liu, C., Widmer, G., Tzipori, S., Buck, G., Xu, P., Bankier, A., Dear, P., Konfortov, B., Spriggs, H., Iyer, L., Anantharaman, V., Aravind, L. & Kapur, V. 2004. Complete genome sequence of the apicomplexan, *Cryptosporidium parvum*. *Science*, **304**:441-445.

Cai, X., Fuller, A., McDougald, L. & Zhu, G. 2004. Apicoplast genome of the coccidian *Eimeria tenella*. *Gene*, **321**:39-46.

Carreno, R., Martin, D. & Barta, J. 1999. *Cryptosporidium* is more closely related to the gregarines than to coccidia as shown by phylogenetic analysis of apicomplexan

parasites inferred using small-subunit ribosomal RNA gene sequences. *Parasitol. Res.*, **85**:899-904.

Escalada, M., Russell, A., Maillard, J. & Ochs, D. 2005. Triclosan-bacteria interactions: single or multiple target sites? *Lett. Appl. Microbiol.*, **41**:476-481.

Fast, N., Kissinger, J., Roos, D. & Keeling, P. 2001. Nuclear-encoded, plastid-targeted genes suggest a single common origin for apicomplexan and dinoflagellate plastids. *Mol. Biochem. Evol.*, **18**:418-426.

Gardner, M., Bishop, R., Shah, T., de Villiers, E., Carlton, J., Hall, N., Ren, Q., Paulsen , I., Pain, A., Berriman, M., Wilson, R., Sato, S., Ralph, S., Mann, D., Xiong, Z., Shallom, S., Weidman , J., Jiang, L., Lynn, J., Weaver, B., Shoaibi, A., Domingo, A., Wasawo, D., Crabtree, J., Wortman, J., Haas, B., Angiuoli, S., Creasy, T., Lu, C., Suh, B., Silva, J., Utterback, T., Feldblyum, T., Pertea, M., Allen, J., Nierman, W., Taracha, E., Salzberg, S., White, O., Fitzhugh, H., Morzaria, S., Venter, J., Fraser, C. & Nene, V. 2005. Genome sequence of *Theileria parva*, a bovine pathogen that transforms lymphocytes. *Science*, **309**:134-137.

Harwood, J. 1996. Recent advances in the biosynthesis of plant fatty acids. *Biochim. Biophys. Acta.*, **1301**:7-56.

Hijjawi, N., Meloni, B., Ryan, U., Olson, M. & Tamavo, S. 2002. Successful *in vitro* cultivation of *Cryptosporidium andersoni*: evidence for the existence of novel extracellular stages in the life cycle and implications for the classification of *Cryptosporidium*. *Internat. J. Parasitol.*, **32**:1719-1726.

Hopkins, J., Fowler, R., Krishna, S., Wilson, I., Mitchell, G. & Bannister, L. 1999. The plastid in *Plasmodium falciparum* asexual blood stages: a three-dimensional ultrastructural analysis. *Protist*, **150**:283-295.

Huang, J., Mullapudi, N., Lancto, C., Scott, M., Abrahamsen, M. & Kissinger, J. 2004. Phylogenomic evidence supports past endosymbiosis, intracellular and horizontal gene transfer in *Cryptosporidium parvum*. *Genome Biol.*, **5**:R88.

Kohler, S. 2005. Multi-membrane-bound structures of Apicomplexa: I. the architecture of the *Toxoplasma gondii* apicoplast. *Parasitol. Re.s*, **96**:258-272.

Kohler, S., Delwiche, C., Denny, P., Tilney, L., Webster, P., Wilson, R., Palmer, J. & Roos, D. 1997. A plastid of probable green algal origin in apicomplexan parasites. *Science*, **275**:1485-1489.

Lang-Unnasch, N., Reith, M., Munholland, J. & Barta, J. 1998. Plastids are widespread and ancient in parasites of the phylum Apicomplexa. *Internat. J. Parasitol.*, **28**:1743-1754.

Leander, B., Clopton, R. & Keeling, P. 2003. Phylogeny of gregarines (Apicomplexa) as inferred from small-subunit rDNA and beta-tubulin. *Int. J. Syst. Evol. Microbiol.*, **53**:345-354.

McFadden, G., Reith, M., Munholland, J. & Lang-Unnasch, N. 1996. Plastids in human parasites. *Nature*, **381**:482.

McFadden, G. & van Dooren, G. 2004. Evolution: red algal genome affirms a common origin of all plastids. *Curr. Biol.*, **14**:R514-516.

McLeod, R., Muench, S., Rafferty, J., Kyle, D., Mui, E., Kirisits, M., Mack, D., Roberts, C., Samuel, B., Lyons, R., Dorris, M., Milhous, W. & Rice, D. 2001. Triclosan

inhibits the growth of *Plasmodium falciparum* and *Toxoplasma gondii* by inhibition of apicomplexan Fab I. *Int. J. Paraitol.*, **31**:109-113.

Obornik, M., Jirku, M., Slapeta, J., Modry, D., Koudela, B. & Lukes, J. 2002. Notes on coccidian phylogeny, based on the apicoplast small subunit ribosomal DNA. *Parasitol. Res.,* **88**:360-363.

Omoto, C., Toso, M., Tang, K. & Sibley, L. 2004. Expressed sequence tag (EST) analysis of gregarine gametocyst development. *Int. J. Paraitol.*, **34**:1261-1271.

Riordan, C., Ault, J., Langreth, S. & Keithly, J. 2003. *Cryptosporidium parvum* Cpn60 targets a relict organelle. *Curr. Genet.,* **44**:138-147.

Rosales, M., Cordon, G., Moreno, M., Sanchez, C. & Mascaro, C. 2005. Extracellular like-gregarine stages of *Cryptosporidium parvum*. *Acta. Trop.*, **95**:74-78.

Ryall, K., Harper, J. & Keeling, P. 2003. Plastid-derived Type II fatty acid biosynthetic enzymes in chromists. *Gene*, **14**:139-148.

Surolia, N. & Surolia, A. 2001. Triclosan offers protection against blood stages of malaria by inhibiting enoyl-ACP reductase of *Plasmodium falciparum*. *Nat. Med.*, **7**:167-173.

Waller, R., Keeling, P., Donald, R., Striepen, B., Handman, E., Lang-Unnasch, N., Cowman, A., Besra, G., Roos, D. & McFadden, G. 1998. Nuclear-encoded proteins target to the plastid in *Toxoplasma gondii* and *Plasmodium falciparum*. *Proc. Natl. Acad. Sci. U S A.*, **95**:12352-12357.

Wilson, R., Denny, P., Preiser, P., Rangachar, K., Roberts, K., Roy, A., Whyte, A., Strath, M., Moore, D., Moore, P. & Williamson, D. 1996. Complete gene map of

the plastid-like DNA of the malaria parasite *Plasmodium falciparum*. *J. Mol. Biol.*, **216**:155-172.

Xu, P., Widmer, G., Wang, Y., Ozaki, L., Alves, J., Serrano, M., Puiu, D., Manque, P., Akiyoshi, D., Mackey, A., Pearson, W., Dear, P., Bankier, A., Peterson, D., Abrahamsen, M., Kapur, V., Tzipori, S. & Buck, G. 2004. The genome of *Cryptosporidium hominis*. *Nature*, **431**:1107-1112.

Zhu, G. 2004. Current progress in the fatty acid metabolism in *Cryptosporidium parvum*. *J. Eukaryot. Microbiol.*, **51**:381-388.

Zhu, G., Marchewka, M. & Keithly, J. 2000a. *Cryptosporidium parvum* appears to lack a plastid genome. *Microbiology*, **146**:315-321.

Zhu, G., Marchewka, M., Woods, K., Upton, S. & Keithly, J. 2000b. Molecular analysis of a Type I fatty acid synthase in *Cryptosporidium parvum*. *Mol. Biochem. Parasitol.*, **5**:253-260.

Table **1**. PCR Primers

| **primer** | **Genes** | **F Primer** | **R primer** | ***B.*** | ***G.*** | Ref |
|---|---|---|---|---|---|---|
| **1** | Plastid LSU rRNA | CTGAATCATCTTAGTACTCAAAG | A(A/G)TGAGCT(T/A)TTACGCACTCTT | + | - | 1 |
| **2** | Plastid LSU rRNA | ATT(T/G)TCAA(A/G)AGGGAACAGCC | TTACACCTTTC(G/A)TGC(G/A)GGTC | + | - | 1 |
| **3** | Plastid LSU rRNA | GCGAAATTCCTGTCGGGTAAGTCC | TTT(C/T)(C/T)G(A/G)TCCTCTCGTACT | + | - | 1 |
| **4** | Plastid SSU rRNA | AGAGTTTGATCCTGGC | TACCTTGTTACGACTT | + | - | 1 |
| **5** | Plastid SSU rRNA | AGGATTAGATACCC | TACCTTGTTACGACTT | + | - | 1 |
| **6** | Plastid tufA-tRNA | CATGT(A/T)GATCATGG(A/T)AAAAC | GGTAGAGCAATGGATTGAAG | + | - | 1 |
| **7** | Nuclear LSU rRNA | TCCTGAGGGAAACTTCGGAGG | GATAGCAACAAGTACCGTGAGG | + | + | 2 |

Amplicons produced (+) or not produced (-) with *B – Babesia equi* DNA , *G – Gregarina niphandrodes* DNA

1. Zhu et. al. 2000a, 2. This study

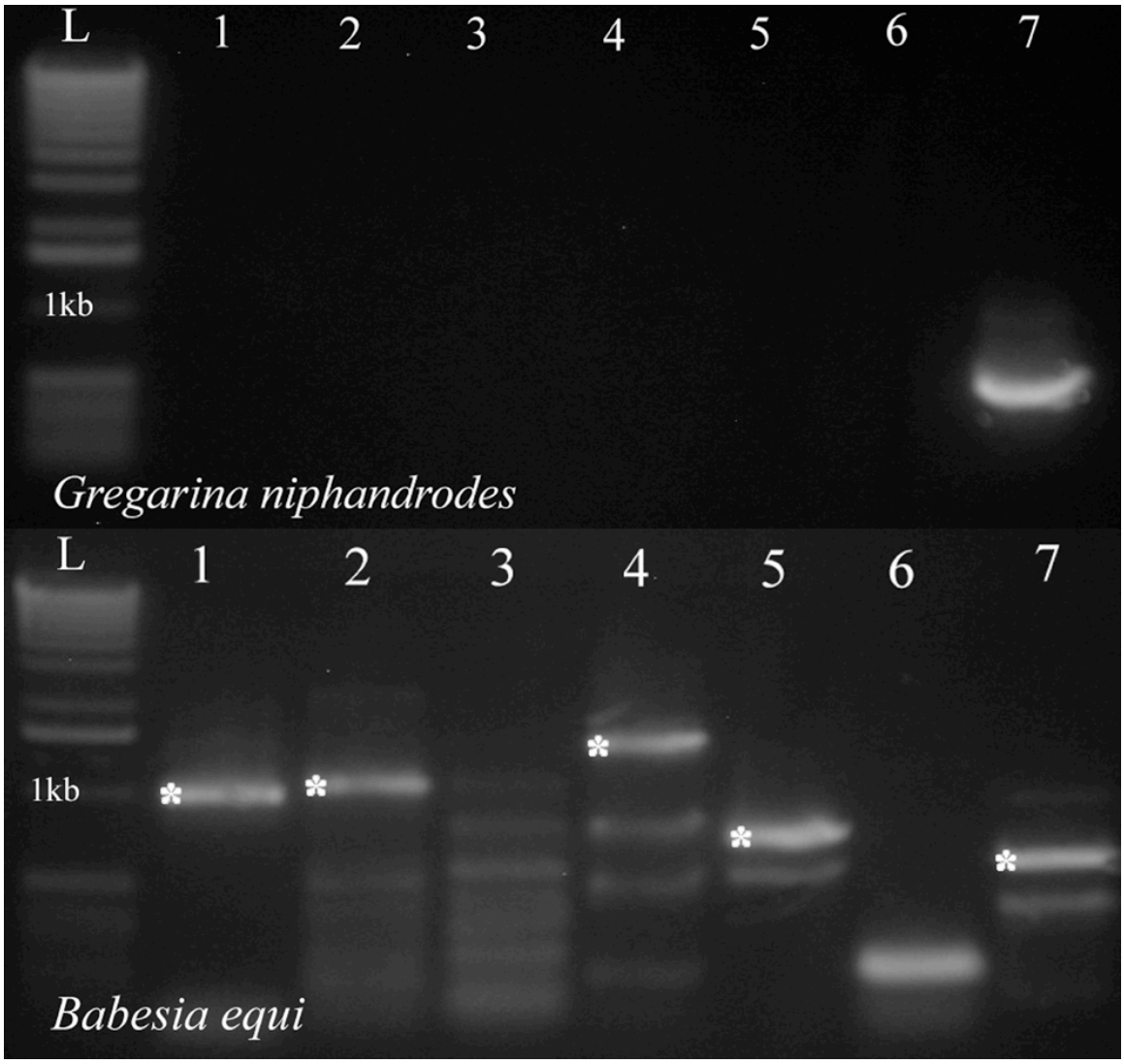


Fig. **1**. Agarose gel of PCR products. No amplicons were produced with plastid-specific primers using DNA from *Gregarina niphandrodes* as template (upper row, Lanes 1--6) whereas all of the primer pairs produced amplicons using *B. equi* DNA template (lower row, Lanes 1--6). Only the large subunit (LSU) rRNA primers produced an amplicon with *G. niphandrodes* DNA (Lane 7). Numbers correspond to primer pairs listed in Table 1. Plastid-specific primers (lanes 1--6), nuclear LSU rRNA primers (lane 7), L, a 1kb ladder, the 1kb band is labeled. * indicates bands that were re-amplified and sequenced.

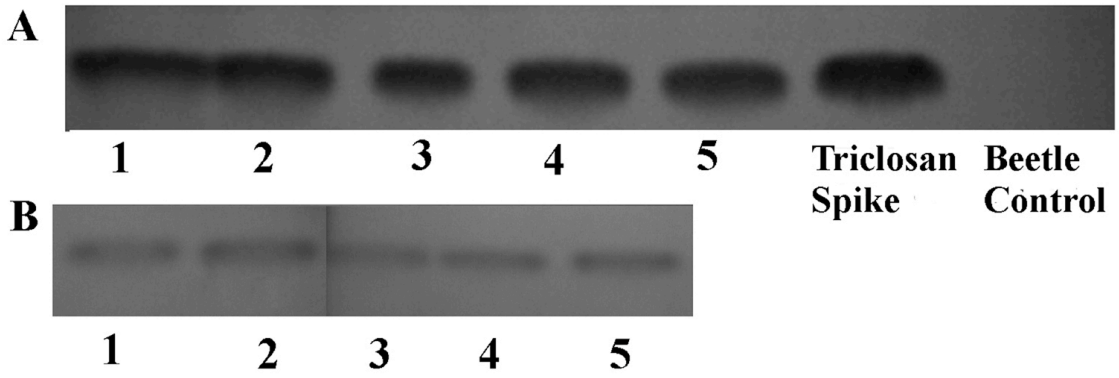


Fig. **2**. Triclosan extracted from the intestines of *Tenebrio molitor* using thin layer chromatography. (A) Seven intestines derived from beetles exposed to triclosan at 4.0 mg/g bran (Lanes 1--5), a triclosan spike of 1.5 _g (Lane 6), and an acetone control (Lane 7). (B) Five intestines from beetles exposed to triclosan at 0.4 mg/g of bran.

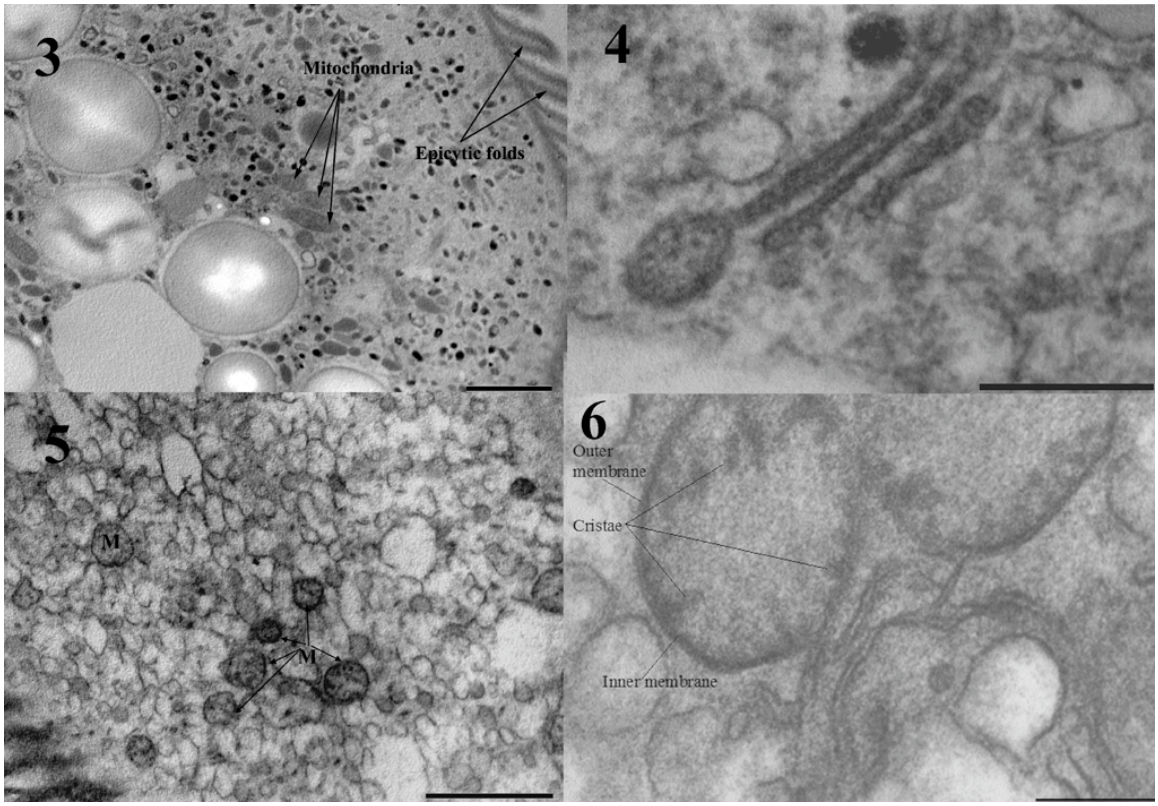


Fig. **3--6**. Transmission election micrographs (TEM) of trophozoites of *Gregarina niphandrodes* fixed with paraformaldehyde and glutaraldehyde (3, 4) and with permanganate (5, 6). **3**. Mitochondria and epicytic folds are clearly seen. Scale Bar-1 μm. **4.** Higher magnification TEM of *G. niphandrodes* showing a Golgi complex. Scale bar-0.2μm. **5.** Numerous mitochondria (M) are visible. Scale bar-1 μm. **6.** Higher magnification TEM of *G. niphandrodes* mitochondria. Outer membrane, inner membrane, and cristae are visible. Bar-200 nm.

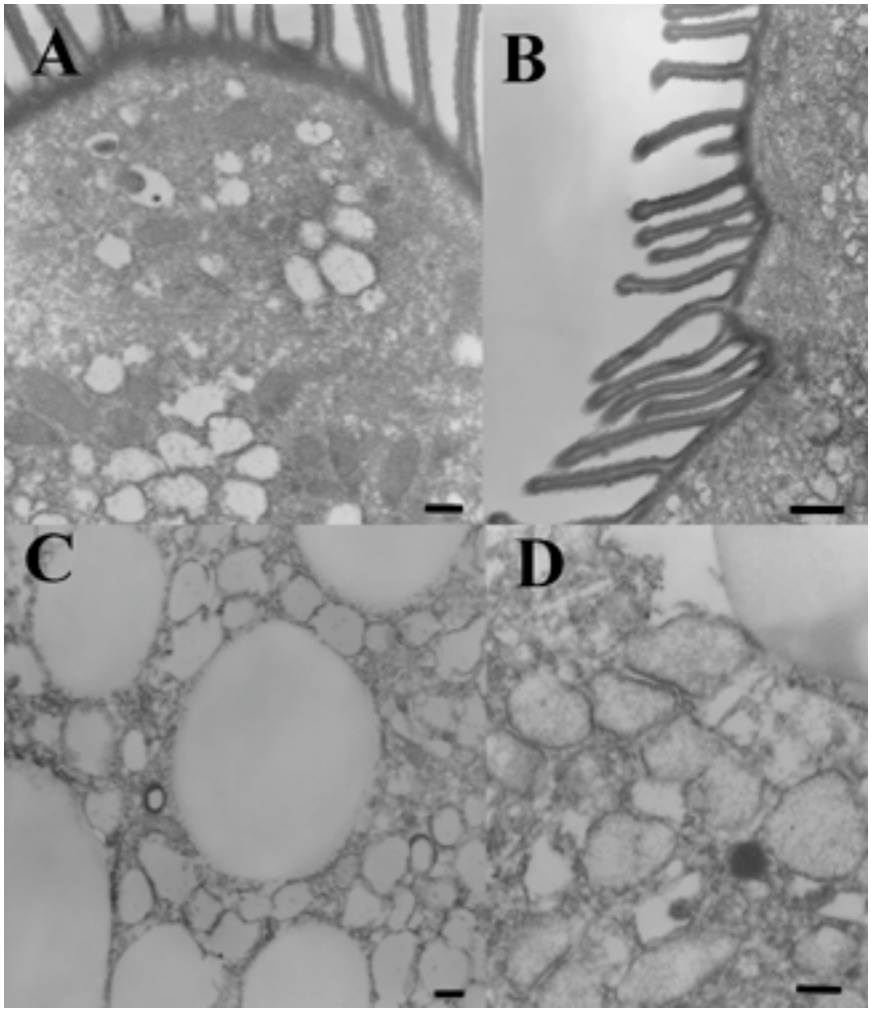


Fig. 7. TEM examples of cytoplasm (A,C & D) and epicytic folds (B) of *G. niphandrodes*. A Scale bar-200nm. B Scale bar-500nm. C Scale bar- 200nm. D Scale bar-200nm

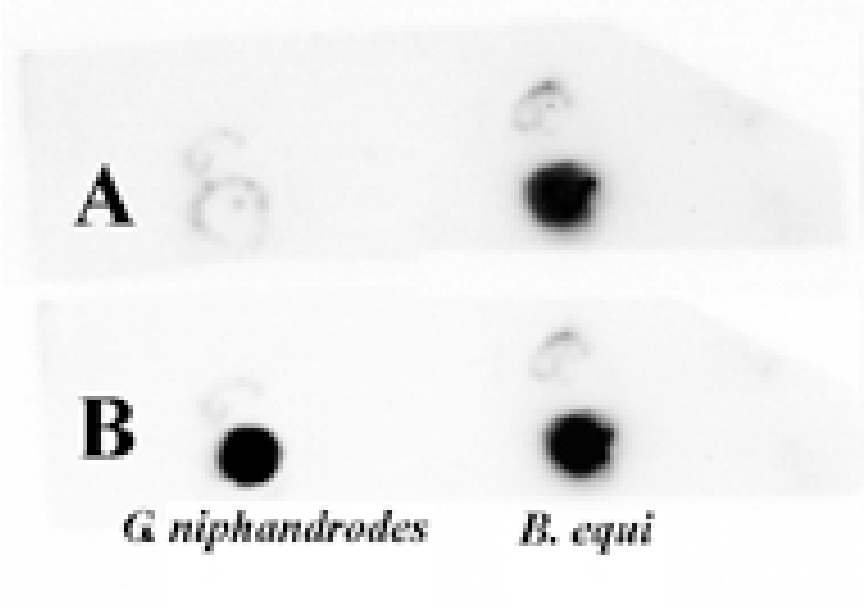


Fig. **8**. Dot-blot of DNA from *Gregarina niphandrodes* and *Babesia equi*. **A**) A mixture of large subunit (LSU) and small subunit (SSU) apicoplast sequences from *B. equi* were used as a probe (see PCR products 1, 2, 4, and 5, Fig. 1). DNA from *B. equi* gave a strong signal while *G. niphandrodes* DNA did not produce any signal. **B**) The nuclear LSU sequence from *G. niphandrodes* as a probe (PCR product 7, Fig. 1) gave very strong signals to both *G. niphandrodes* and *B. equi* DNA.

CHAPTER TWO

# ULTRASTRUCTURE OF *GREGARINA NIPHANDRODES* NUCLEUS THROUGH STAGES FROM UNASSOCIATED TROPHOZOITES TO SPHERICAL GAMONTS AND THE SYZYGY JUNCTION.

**MARC A. TOSO and CHARLOTTE K. OMOTO***

School of Biological Sciences, Washington State University, Pullman, Washington 99164-4236, USA *e-mail:omoto@wsu.edu*

[Formatted for the Journal of Parasitology]

**ABSTRACT:** In *Gregarina niphandrodes*, an apicomplexan parasite, the sexual stage of its life cycle begins with syzygy. Here, we describe the ultrastructure of the syzygy junction and the nucleus during the transition from unassociated trophozoites to trophozoites in syzygy to spherical gamonts in syzygy. Throughout this process, the folds within the syzygy junction undergo changes that correspond to changes of the epicytic folds. The nucleus goes through dramatic changes from multiple spheres of condensed chromatin in unassociated trophozoites, to mostly uncondensed chromatin in trophozoites in syzygy to a large single sphere of condensed chromatin encasing many smaller spheres in spherical gamonts. These differing nuclear ultrastructures reflect the dramatic cellular and transcriptional changes associated with life cycle transitions and are indicative of the numerous cell divisions to follow.

INTRODUCTION

Gregarines are in the phylum Apicomplexa, which consists of obligate parasites. Gregarines are of no medical importance and consequently are understudied unlike species of *Plasmodium, Toxoplasma, Cryptosporidium, Eimeria,* and *Babesia*. The eugregarine, *Gregarina niphandrodes,* is easily maintained in the laboratory in its host, *Tenebrio molitor,* the yellow mealworm beetle. *Gregarina niphandrodes* has a monoxenous life cycle in which a haploid sporozoite is consumed by an adult *Tenebrio. molitor*. The sporozoite travels to the intestine where it grows into a large (between 0.1-0.2 mm in length) trophozoite, the feeding stage of the life cycle. Trophozoites have 2 main compartments, the smaller head-like protomerite and the larger deutomerite plus a smaller epimerite (Clopton, et al., 1991). The sexual stage of the life cycle begins with syzygy, when one trophozoite's protomerite connects to the base of its partner's deutomerite (Fig. 1). After making this connection, both trophozoites lose their oblong shape and become spherical gamonts. The gamonts then encase themselves within a tough gametocyst wall; at this stage, they are shed with the host frass. Multiple cell divisions and differentiation result in male and female gametes. Mixing of the gametes is followed by fertilization. The diploid zygote undergoes meiosis followed by mitosis to form haploid sporozoites within oocysts that are released from the gametocyst in chains.

A number of ultrastructural investigations of gregarines have shown the role of microtubules during the sexual stage (Kuriyama et al., 2005), actin and myosin (Chen and Fan-Chiang, 2001; Heintzelman, 2004), and epicytic folds in trophozoites (Reger, 1967; Schrevel et al., 1983). The structure of trophozoites in syzygy of eugregarines *Gregarina*

*polymorpha* (Devauchelle, 1968), *Gregarina rigida* (Beams et al., 1959), and *Pterospora floridiensis* (Landers, 2002), and the archigregarine *Selenidium pennatum* (Kuvardina and Simdyanov, 2002) have been studied, but little is known regarding the transition from unassociated trophozoites to cells in syzygy. Many ultrastructural observations of the gregarine nuclei have been made (Walsh and Callaway, 1969; Desportes, 1974; Lucarotti, 2000; Ciancio et al., 2001; Hoshide and Janovy, 2002); however, there have been few observations comparing the nuclear ultrastructure of different stages. We have undertaken a detailed investigation into the junction between 2 trophozoites and spherical gamonts during syzygy and the transformation of the nuclear structure from unassociated trophozoites to spherical gamonts.

## MATERIALS AND METHODS

### Transmission electron microscopy

*Tenebrio molitor* intestines were dissected in insect Ringer's solution (120 mM NaCl, 1.2 mM KCl, 1.4 mM $CaCl_2$) and unassociated *G. niphandrodes* trophozoites, trophozoites in syzygy, and spherical gamonts in syzygy were fixed overnight at 4 C in 2% paraformaldehyde and 2% glutaraldehyde in 0.1 M cacodylate buffer. Samples were rinsed 3 times in 0.1 M cacodylate buffer prior to a 2-hr post-fixation with 2% osmium tetroxide in 0.1 M cacodylate buffer. They were rinsed 3 times in distilled $H_2O$ and stained in 1% tannic acid for 1 hr. The specimens were dehydrated in an acetone series and embedded in Spurr's resin. Ultrathin sections (70 nm) were cut with a glass knife on a Leica Reichert microtome and placed on formvar coated copper grids. Grids were stained with uranyl acetate and Sato's lead and viewed on a JEOL 1200 EX TEM. Photos

were processed with Photoshop 5.0. All measurements were performed with NIH ImageJ 1.34S.

**Light microscopy**

Unassociated trophozoites, trophozoites in syzygy, and spherical gamonts in syzygy were harvested and processed as described above and also embedded in Spurr's resin; 300 nm sections were obtained using a glass knife and heat dried on a glass slide. Sections were stained for 45 sec with Stevenel's Blue. Staining with Stevenel's blue parallels the electron density of the same material in the electron microscope, and provides excellent differentiation between materials, particularly in the nucleus (del Cerro et al., 1980).

**RESULTS**

**Surface and junctional features**

*Trophozoites:* Within the intestinal lumen of *T. molitor,* 2 trophozoites come together in an act of syzygy (Fig. 1). The protomerite and deutomerite of both cells are visible in this figure as is the junction between the 2 partners. The syzygy junction is a complex structure with an appearance similar to a chain-linked-fence ~1.6_m wide (Fig. 2). The surfaces of the trophozoites are covered in long epicytic folds (Fig. 3) that run the cell's length. Within the syzygy junction, the trophozoites' epicytic folds directly contact each other with the tips of the epicytic folds interlocking (Figs. 2). The epicytic folds of the protomerite surface are the same size as the epicytic folds within the syzygy junction on the protomerite side of the syzygy junction, ~300 nm (Figs. 2 & 4), as do the folds on the deutomerite and the epicytic folds within the syzygy junction on the deutomerite side, ~800 nm (Figs. 2 & 3). An internal lamina (IL) runs basal to both the epicytic folds on

the trophozoites' surfaces and within the syzygy junction (Figs. 2-4). At the tips of both the epicytic folds on the cell's surface and within the syzygy junction are rows of thin, ~10-12 nm, apical filaments (Figs. 2 & 5).

*Spherical gamonts***:** During the next stage of syzygy, the trophozoites undergo dramatic structural transformation. They lose their oblong shape and become spherical prior to the laying down of the gametocyst wall. We refer to them as spherical gamonts (Fig. 6). At this stage, there is a structural change in the junction between the 2 cells and in the epicytic folds. The length of the epicytic folds during this spherical gamont stage is ~200 nm, also a thin membrane appears to stretch between the folds (Fig. 8), this may be the early stages of gametocyst wall formation. The length of folds within the syzygy junction of both gamonts is also, ~200 nm (Fig. 7). The junction between the 2 cells is less compact than in earlier stages of syzygy; there is greater space between the epicytic folds within the syzygy junction of both gamonts (Fig. 7). The ~10-12 nm apical filaments continue to line the epicytic folds within the junction (Fig. 7) as well as on the spherical gamont surface (Fig. 8).

**Nucleus**

*Trophozoites***:** The trophozoite nucleus is quite large (~22 _m in diameter)(Fig. 9), and has numerous indentations (Fig. 9 & 10). Spherical condensed chromatin is easily observed in a central circular region within the nucleus at the light microscopic level using Stevenel's blue stain and at the electron microscopic level (Figs. 9-11). Both figures 9 & 10 show a large clear circular region framed by the condensed chromatin spheres. The diameter of this central circular region is ~15 μm. The inside of the nuclear membrane is lined with a honeycomb-patterned structure (Fig. 12.)

*Trophozoites in syzygy:* Concavities within the nuclear membrane are visible on the nucleus of trophozoites in syzygy (Fig. 13). There was partly decondensed chromatin organized in several areas throughout the nuclei (Fig. 13). Nuclei of 3 couples in syzygy were sectioned through in their entirety and examined at the light microscopic level and no spherical condensed chromatin was observed (Fig. 1) Honeycomb-patterned structures within the nuclei were also observed in the nuclei of trophozoites in syzygy (Figs. 14 & 15).

*Spherical gamonts:* The spherical gamont nuclei are also large and easily seen in light microscopy (Fig 16). A large sphere of condense chromatin (~10 μm diameter) was always observed at the periphery of the nuclei (Fig. 16). Many smaller spheres of dense chromatin are visible within this dense sphere of chromatin. These smaller spheres were visible using Stevenel's blue stain at the light microscopic level (Fig. 16) and at the electron microscopic level (Fig. 17). Four (Fig. 17) to 19 (Fig. 16) small spheres varying in size from ~90 $nm^2$-1.5 _$m^2$ were observed, depending upon the section plane. At this stage, the inner lining of the nuclear membrane lacked the honeycomb pattern (Fig. 18).

**DISCUSSION**

In gregarines, syzygy is defined as the stage in which the haploid trophozoites of opposite mating types initiate the processes of sexual reproduction. This process involves major changes in cellular morphology as well as in gene expression. Thus we sought to characterize in detail the cell-cell junction and changes in nuclear morphology during this process.

In *G. niphandrodes*, 2 trophozoites couple together with the protomerite of one cell attaching to the deutomerite of the other cell (Fig. 1). Epicytic folds (Figs. 2 & 3)

characteristic of the surface architecture of many gregarines have been studied in detail (Reger, 1967; Devauchelle, 1968; Schrevel et al., 1983; Heintzelman, 2004). Upon syzygy, the tips of their epicytic folds interlocked tightly in a chain-link like structure (Figs. 2). Epicytic folds both within and outside the syzygy junction are multimembranous structures underlain by internal lamina with ~10-12 nm filaments at their apical aspect (compare Figs. 2 & 3 with Figs. 7 & 8). The lengths of the epicytic folds within the junction correspond to their length outside the junctional region.

The structure of the syzygy junction in spherical gamonts is similar to that of trophozoites in syzygy. During both stages, the epicytic folds within the syzygy junction reflect the structure of surface epicytic folds. Within the syzygy junction of spherical gamonts, the epicytic folds are reduced in size compared to trophozoites in syzygy. Within the syzygy junction, the size of the epicytic folds corresponds to the epicytic folds on the surface of the spherical gamonts. Also the epicytic folds in the syzygy junction of spherical gamonts are less compact than trophozoites in syzygy. Trophozoites in syzygy have electron dense material sandwiched between the epicytic folds in the junction, while this is lacking in spherical gamonts (Fig. 7)

Similar interlocking of the epicytic folds' tips during syzygy of trophozoites in other eugregarines has been observed (Beams et al., 1959; Devauchelle, 1968). In *G. rigida* trophozoites in syzygy (Beams et al., 1959), it was speculated that droplets of darkly stained mucus hold the trophozoites together in syzygy. In micrographs of *G. polymorpha* trophozoites in syzygy (Devauchelle, 1968), the interlocking tips of the epicytic folds are present, yet no vesicles or mucus droplets were noted. Interestingly, epicytic folds are lacking in gregarines that do not exhibit gliding movement, like the

Selenidiidae, an archigregarine (Schrevel et al., 1983). Syzygy has been studied in *Selenidium pennatum* by Kuvardina and Simdyanov (2002); however, they observed that the association between the trophozoite partners was unstable and that the dehydration process disrupted them. This was not observed in *G. niphandrodes*; no special precautions were necessary to maintain the association of trophozoites in syzygy. In *G. niphandrodes* and other eugregarines, there is a regular and consistent interlocking of the tips of the epicytic folds (Figs. 2). This would provide a large surface area for stable interactions that may help bind the trophozoites together that perhaps the Selenidiidae lack.

The eugregarine *Pterospora floridiensis* lacks epicytic folds and instead has epicytic ridges, which lack the apical filaments observed in epicytic folds. In contrast to the tips of the epicytic folds interlocking, the majority of those junction is pressed together flatly (Landers, 2002). The interactions between the associated trophozoites within this junction may hold the syzygy intact. In these gregarines, trophozoites form syzygy early, so it is unknown if there is a structural change in the region where the junction occurs in the transformation of unassociated trophozoites to associated trophozoites/gamonts in syzygy (Landers, 2002).

The transition of *G. niphandrodes* from a large single trophozoite actively feeding and metabolizing to association of 2 cells to begin the sexual stage to form many gametes within a gametocyst requires dramatic changes in cellular activity. These changes must involve major changes in nuclear activity and is accompanied by structural transformation of the nucleus. The chromatin in *G. niphandrodes* nucleus has distinct structures in each of the 3 observed stages: unassociated trophozoites, trophozoites in

syzygy, and the spherical gamonts in syzygy. The unassociated trophozoite nuclei have spheres of tightly condensed chromatin which frame a central circular region, and the nuclei of trophozoites in syzygy have mostly uncondensed chromatin. However, some darker regions of more condensed chromatin were also observed. The spherical gamonts possess a single condensed chromatin sphere containing smaller dense spheres, while the rest of the nuclei have a homogeneous appearance. The variation in chromatin structure in these stages of *G. niphandrodes* may reflect changes in transcription and preparation for nuclear division.

Within unassociated trophozoites' nuclei, many spheres of condensed chromatin are visible (Figs. 9 -11). These spheres are then arranged in a circular region within the nucleus (Fig. 9 & 10). These observations are very different from the nuclei observed in the unassociated eugregarine trophozoites *Lankesteria culicis* and *Lankesteria ascidiae*, which possess large nucleoli with finely dispersed chromatin (Walsh and Callaway, 1969; Ciancio et al., 2001). Hoshide and Janovy (2002) observed many round nucleoli in the trophozoite of *Odonaticola polyhamatus*. However, they were scattered throughout the nuclei and lacked the organized circular region present in *G. niphandrodes.* The nuclei of unassociated trophozoites of the eugregarine *Leidyana canadensis* sometimes divides many times prior to the pairing of trophozoites in syzygy (Lucarotti, 2000). This was not observed in *G. niphandrodes,* which possesses a single large nucleus through all stages, from unassociated large trophozoite to spherical gamont.

The honeycomb pattern we found on the inner lining of nuclei in both unassociated trophozoites and trophozoites in syzygy have been observed in several other unassociated gregarine trophozoites (Beams et al., 1957; Desportes, 1974; Hoshide and

Janovy, 2002). The latter authors (Hoshide and Janovy, 2002) have suggested the honeycomb layer may provide structural support for the nucleus.

During the initial stages of syzygy, the condensed chromatin within the trophozoite appears more dispersed throughout the nucleus (Fig. 13). Syzygt is the beginning of dramatic changes in cellular activity and in transcriptional activity. The changes in nuclear morphology may be necessary to facilitate this transformation. Two concavities were observed in the nucleus (Fig. 13). Similar concavities are have been observed in *Lecudina tuzetae* gametocysts, possibly due to the forces of growing microtubules (Kuriyama et al., 2005). These concavities within the trophozoites in syzygy indicates that processes that lead to the concavity must begin earlier in *G. niphandrodes*. There are few other observations of the nuclei during this stage. Devauchelle (1968) and Beams et al. (1957) examined syzygy, but made no observations of the nuclear structure. Syzygy has also been studied in the archigregarine *Selenidium pennatum*, but nuclear structure was not reported (Kuvardina and Simdyanov, 2002). After the formation of the gametocyst wall, the nucleus replicates hundreds of times to form many haploid nuclei, which, in turn, become nuclei for hundreds of male and female gametes. In this study, we observed that the chromatin condenses into a dense sphere just prior to the formation of the gametocyst wall. Within this dense sphere, 4-19 smaller spheres can be seen, depending upon the section plane (Figs. 16 & 17). The nuclei in the spherical gamonts are very different from those of unassociated trophozoites and trophozoites in syzygy. The honeycomb structure present in trophozoites is absent in the spherical gamonts (Fig. 18). If this honeycomb layer does provide structural support, then its absence in spherical gamonts may be a prerequisite for the hundreds of nuclear

divisions that are about to occur in the following gametocyst stage.

**ACKNOWLEDGMENTS**

We thank the WSU Franceschi Microscopy and Imaging Center, namely Chris Davitt, Valerie Lynch-Holm and the late Vince Franceschi for assistance and guidance in microcopy. Dr. John Janovy, University of Nebraska, Lincoln, for instruction with *T. molitor* and gregarine care.

**Literature Cited**

Beams, H., T. Tahmisian, R. Devine, and E. Anderson, E. 1957. Ultrastructure of the nuclear membrane of a gregarine parasitic in grasshoppers. Experimental Cell Research **13:** 200-204.

_____, _____, _____, and _____. 1959. Studies on the fine structure of a gregarine parasitic in the gut of the grasshopper, *Melanoplus differentialis*. Journal of Protozoology **6:** 136-146.

Chen, W., and M. Fan-Chiang. 2001. Directed migration of *Ascogregarina taiwanensis* (Apicomplexa: Lecudinidae) in its natural host *Aedes albopictus* (Diptera: Culicidae). Journal of Eukaryotic Microbiolgy **48:** 537-541.

Ciancio, A., S. Scippa, and M. Cammarano. 2001. Ultrastructure of trophozoites of the gregarine *Lankesteria ascidiae* (Apicomplexa : Eugregarinida) parasitic in the ascidian *Ciona intestinalis* (Protochordata). European Journal of Protistology **37:** 327-336.

Clopton, R., T. Percival, and J. Janovy. 1991. *Gregarina niphandrodes* N. Sp. (Apicomplexa: Eugregarinorida) from adult *Tenebrio molitar* (L.) with oocyst descriptions of other gregarine parasites of the yellow mealworm. Journal of Protozoology, **38:** 472-479.

del Cerro, M., J. Cogen, and C. del Cerro. 1980. Stevenel's Blue, an excellent stain for optical microscopical study of plastic embedded tissues. Microscopica acta **83:** 117-121.

Desportes, I. 1974. Ultrastructure et evolution nucleaire des trophozoites d'une gregarine d'ephemeroptere: *Enterocystis fungoides* Codreanu. Journal of Protozoology **21:** 83-94.

Devauchelle, G. 1968. Study of the ultrastructure of *Gregarina polymorpha* (Hamm) in syzygy. Journal of Protozoology **15:** 629-636.

Heintzelman, M. 2004. Actin and myosin in *Gregarina polymorpha*. Cell Motility and the Cytoskeleton **58:** 83-95.

Hoshide, K., and J. Janovy, Jr. 2002. The structure of the nucleus of *Odonaticola polyhamatus* (Gregarinea Actinocephalidea), a parasite of *Mnais strigata*(Hagen) (Odonata:Calopterygidae). Acta Protozoologica **41:** 17-22.

Kuriyama, R., C. Besse, M, Geze, C. Omoto and J. Schrevel. 2005. Dynamic organization of microtubules and microtubule-organizing centers during the sexual phase of a parasitic protozoan, *Lecudina tuzetae* (Gregarine, Apicomplexa). Cell Motility and the Cytoskeleton **62:** 195-209.

Kuvardina, O. and T. Simdyanov. 2002. Fine structure of syzygy in *Selendium pennatum*. Protistology **2:** 169-177.

Landers, S. 2002. The fine structure of the gamont of *Pterospora floridiensis* (Apicomplexa: Eugregarinida). Journal of Eukaryotic Microbiology **49:** 220-226.

Lucarotti, C. 2000. Cytology of *Leidyana canadensis* (Apicomplexa : Eugregarinida) in *Lambdina fiscellaria fiscellaria* larvae (Lepidoptera : Geometridae). Journal of Invertebrate Pathology **75:** 117-125.

Reger, J. 1967. The fine structure of the gregarine *Pyxinoides balani* parasitic in the barnacle *Balanus tintinnabulum*. Journal of Protozoology **14:** 488-497.

Schrevel, J., E. Caigneaux, D. Gros, and M. Philippe. 1983. The three cortical membranes of the gregarines. I. Ultrastructural organization of *Gregarina blaberae*. Journal of Cell Science **61:** 151-174.

Walsh, R.J. and C. Callaway. 1969. The fine structure of the gregarine *Lankesteria culicis* parasitic in the yellow fever mosquito *Aedes aegypti*. Journal of Protozoology **16:** 536-545.

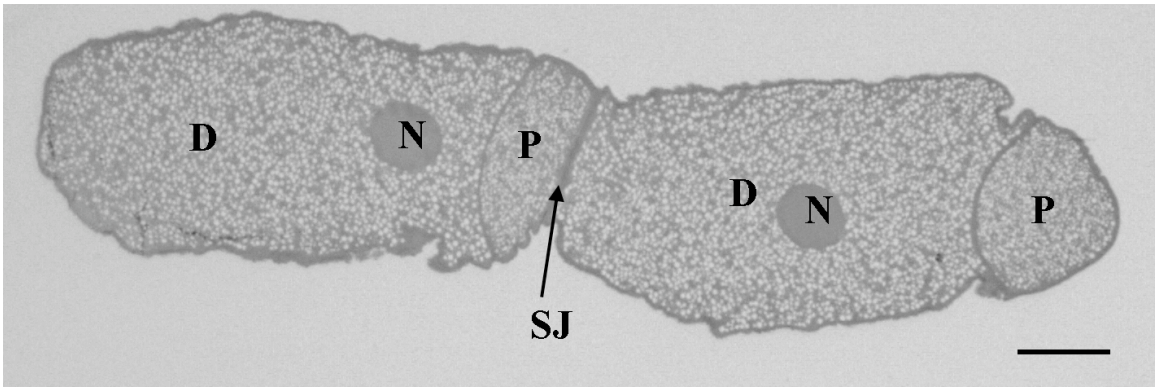


FIGURE. 1. Light micrograph of 2 trophozoites in syzygy. Both cells with their protomerite (P) deutomerite (D) and nucleus (N) are visible. The syzygy junction (SJ) is also visible in this section. Scale Bar 10-_m

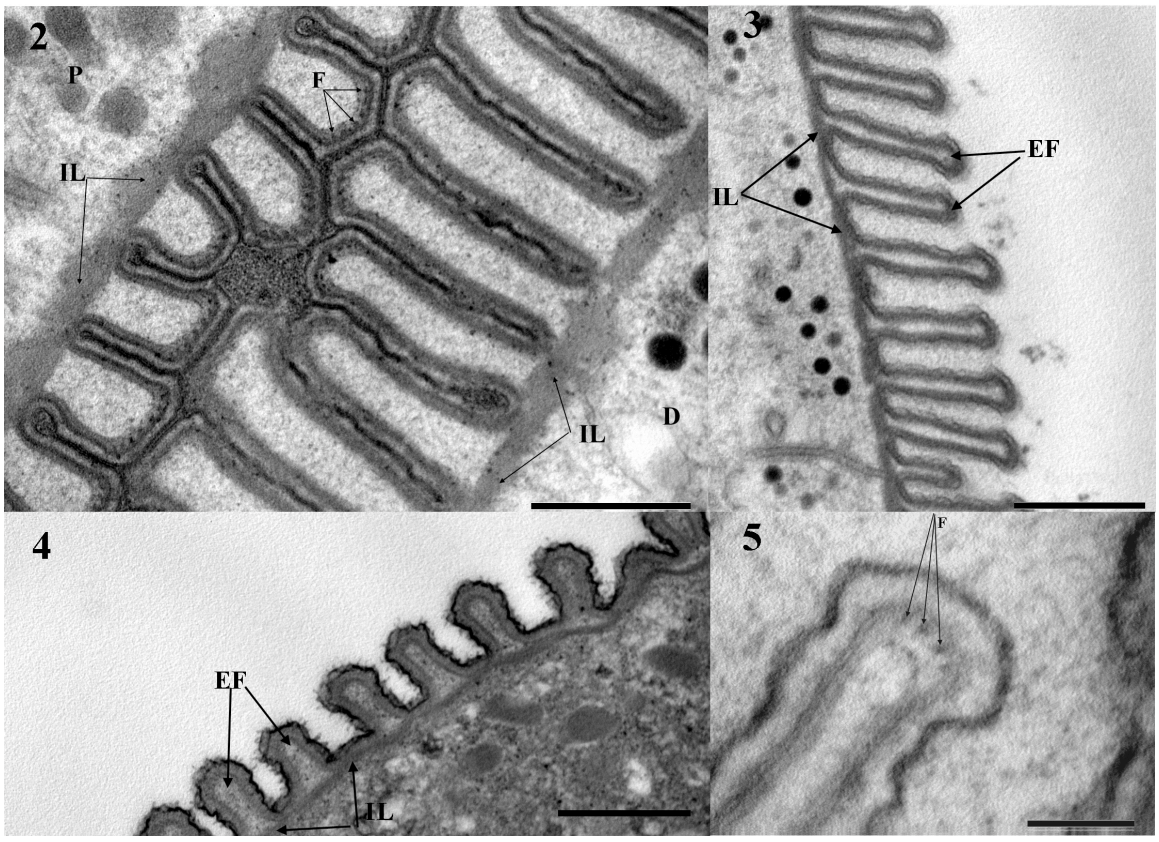


FIGURES. 2-5. Transmission Electron Micrographs (TEM) of syzygy junction and epicytic folds. **(2)** TEM of the syzygy junction. The protomerite (P) and deutomerite (D) are noted. An internal lamina (IL) is visible beneath the folds within the syzygy junction. Filaments (F) are observed in the tips of the folds. Electron dense material is found sandwiched between the folds of coupled cells. Scale bar-0.5_m (**3)** TEM of the epicytic folds (EF) of the deutomerite. The internal lamina (IL) runs basal to the epicytic folds. Scale bar-1_m. (**4)** TEM of epicytic folds on the protomerite. Internal lamina (IL) can be seen basal to the epicytic folds (EF). Scale bar-0.5_m (**5)** Higher magnification TEM of apical filaments (F) in the tip of an epicytic fold. Scale bar-0.1_m

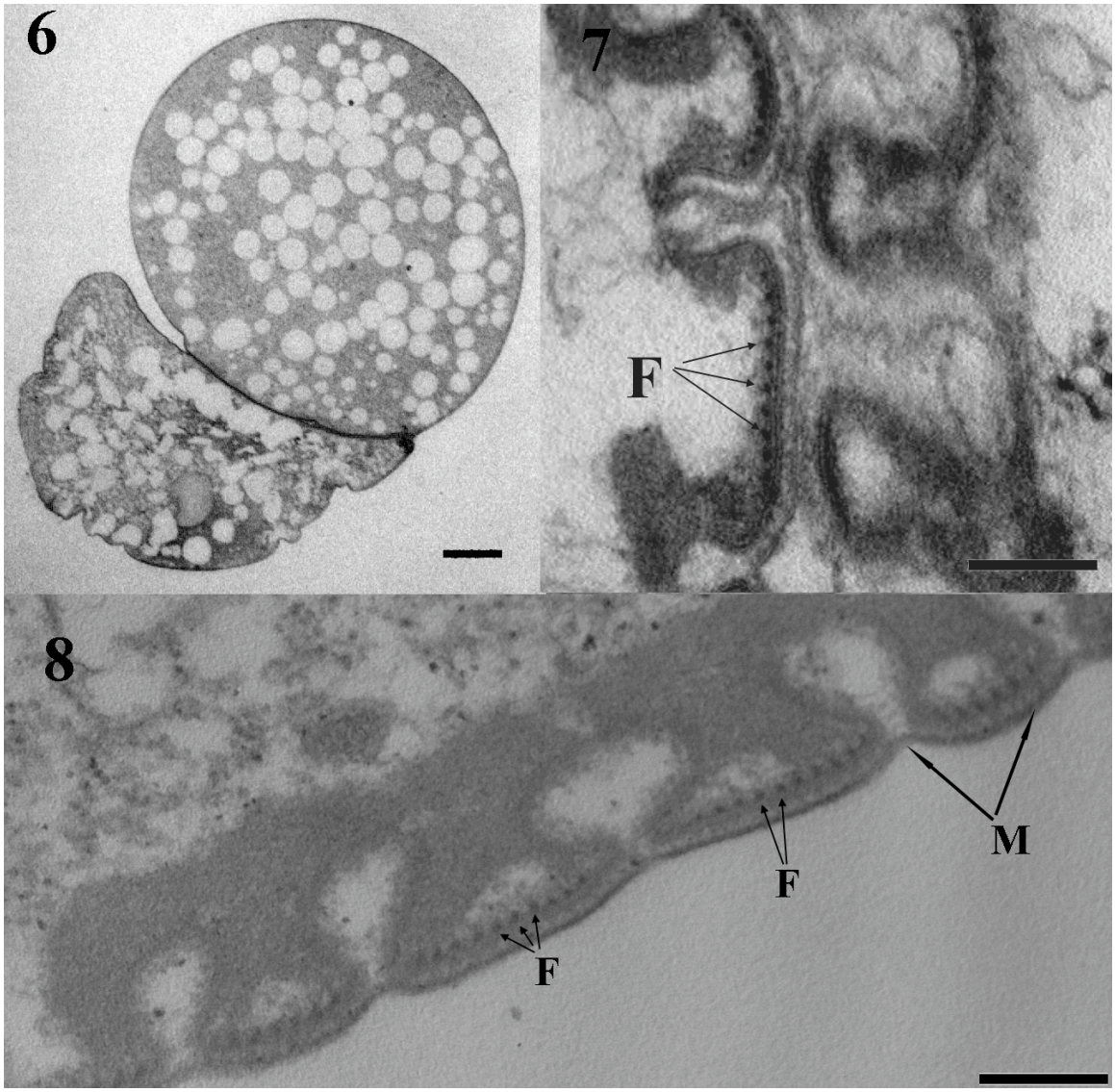


FIGURES 6-8. Micrographs of spherical gamonts stage. **(6)** Light micrograph of syzygy between spherical gamonts. The junction between the gamonts appears dense. Scale bar-500_m. (**7**). Higher magnification TEM of the junction between the 2 spherical gamonts. Apical filaments (F) can be seen under the membrane. Scale bar-0.2_m (**8**). TEM of epicytic folds on a gamont surface. Apical filaments (F) line the tips of the epicytic folds. A continuous outer membrane (M) appears to stretch between the folds. Scale bar-0.2_m

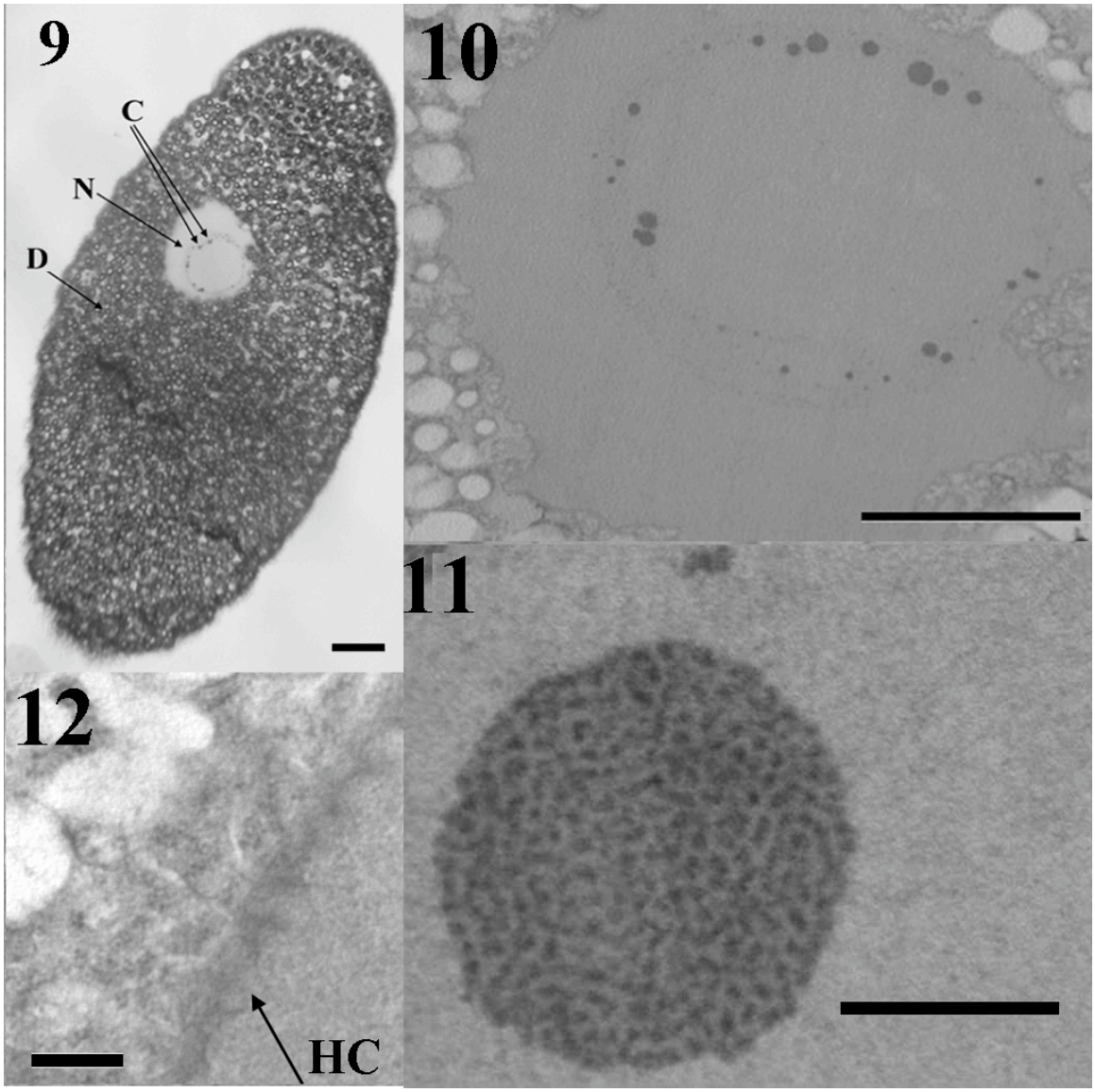


FIGURES 9-12. Micrographs of unassociated trophozoites. (**9**) Light micrograph of an unassociated trophozoite. A large nucleus (N) is found in deutomerite (D). Numerous chromatin (C) are visible with Stevenel's stain. Scale bar-10_m (**10)** TEM of an unassociated trophozoite nucleus showing numerous chromatin spheres framing a central circular region. Scale bar-10_m (**11)** High magnification TEM of a single chromatin sphere Scale bar-0.5 _m (**12)** TEM of a nucleus (N) of an unassociated trophozoite. Honeycomb (HC) structure lines the interior of the nuclear membrane. Scale bar-0.25 μm

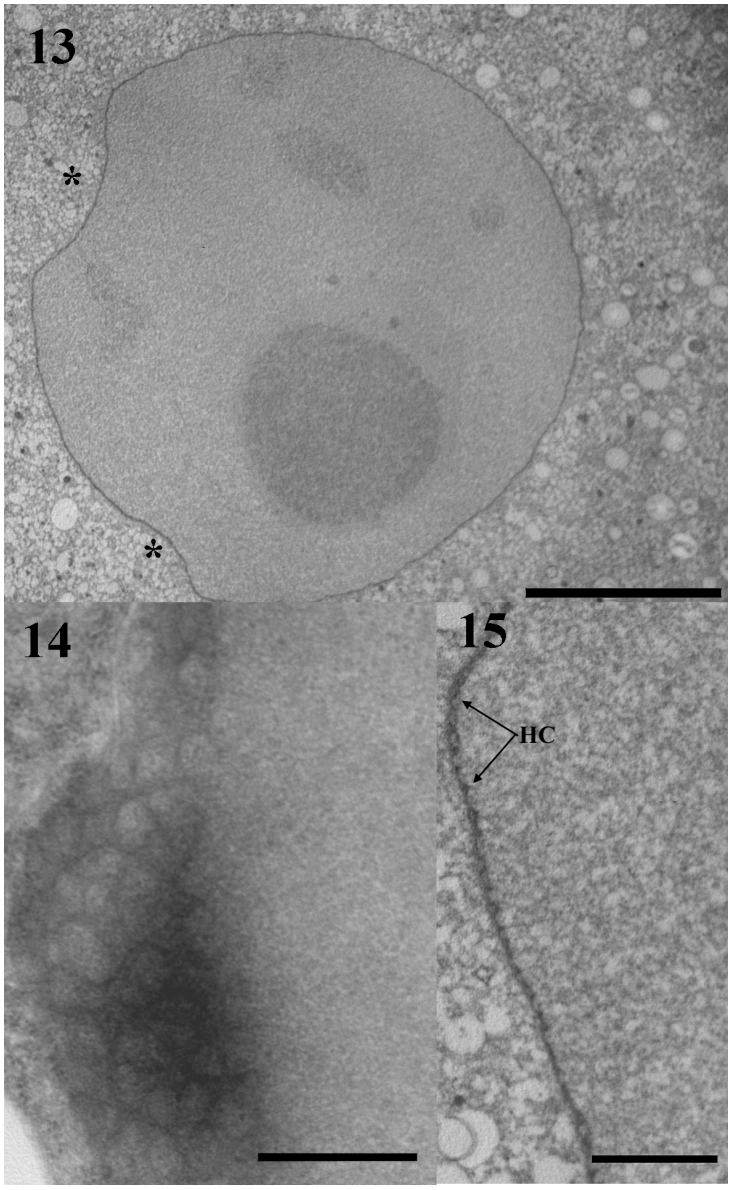


FIGURES 13-15. TEM of nuclear structure of trophozoites in syzygy. **(13)** TEM of nucleus. The chromatin in the nucleus appears more diffuse. Two concavities (*) are visible in the nucleus. Scale Bar-10_m (**14)** Higher magnification tangential section of the honeycomb structure of trophozoite nucleus in syzygy. Scale bar-.5_m (**15)** TEM of a nuclear membrane. Honeycomb (HC) structure lines the interior of the nuclear membrane. Scale bar-1_m

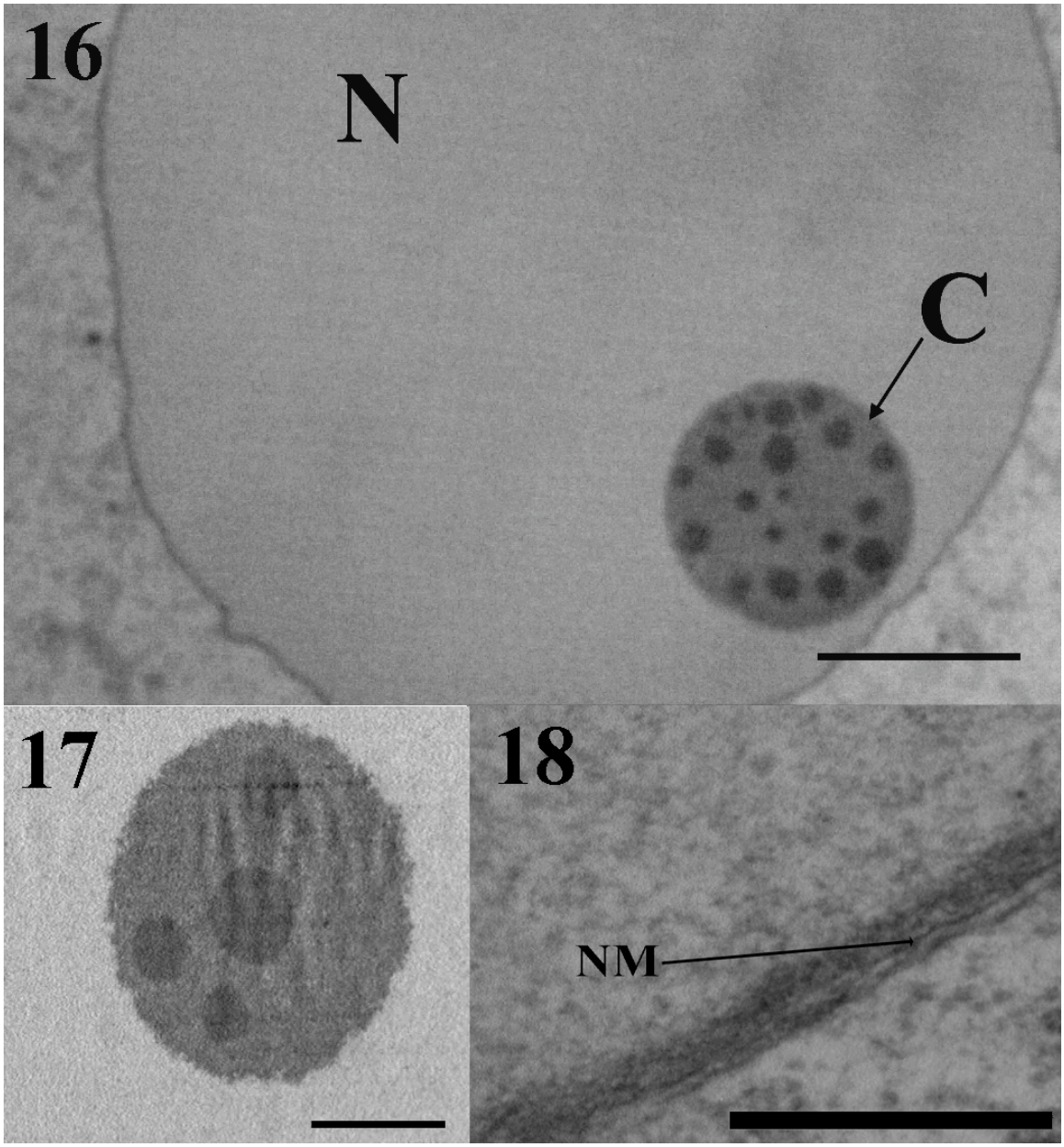


FIGURES 16-18. Micrographs of spherical gamonts. (**16**) Light micrograph of a nucleus (N) containing condensed chromatin (C) spheres. Scale bar-10_m (**17)** Higher magnification TEM of condensed chromatin spheres. Scale bar-2_m **(18**). High magnification TEM of the nuclear membrane (NM). Scale bar-0.2_mbar-2_m **(18**). High magnification TEM of the nuclear membrane of a spherical gamont. Nuclear menbrane (NM). Nucleus (N). Scale bar-0.2_m

## CHAPTER THREE

*Gregarina niphandrodes* possess non-mitochondrial extranuclear DNA

**MARC A. TOSO and CHARLOTTE K. OMOTO**

School of Biological Sciences, Washington State University, Pullman, Washington 99164-4236, USA

[Formatted for the Journal of Eukaryotic Microbiology]

ABSTRACT

Corresponding Author: C.K. Omoto, PO Box 4236,

Washington State University, Pullman, WA 99164-4236

Tel: 509-335-5591; Fax 509-335-3184; Email:omoto@wsu.edu

ABSTRACT

Within the Apicomplexan phylum two species of extranuclear DNA are present: plastid and mitochondrial. However, *Cryptosporidium* has no extranuclear DNA, lacking both the plastid and mitochondrial genome. Gregarines are thought to be sister to *Cryptosporidium*. Organelles identified as "mitochondria" have been observed in both *Cryptosporidium* and gregarines. Gregarine*s* appear to be lacking a plastid genome. It is not known if gregarines possess a mitochondrial genome or any other extranuclear DNA. We used fluorescent microscopy to identify DNA in the cytoplasm and gel electrophoresis to identify DNA that migrated at a faster rate than the nuclear DNA. Using PCR we identified the gene, cytochrome oxidase subunit I, which has been found on every mitochondrial genome sequenced. However, this sequence hybridized to the nuclear DNA during Southern analysis. We cloned and partially sequenced the extranuclear DNA which is believed not to be of mitochondrial origin.

INDTRODUCTION

Gregarines are protozoa in the phylum Apicomplexa. Other more commonly studied organisms within the Apicomplexa are *Cryptosporidium*, *Toxoplasma*, *Plasmodium*, *Babesia*, *Theileria,* and *Eimeria.* Some studies suggest a sister relationship of gregarines with *Cryptosporidium* as well as an early divergence within the phylum based upon the analyses of small-subunit ribosomal RNA (Carreno et al., 1999) (Leander et al., 2003). This sister relationship is supported by similar life-cycle characteristics, namely syzygy and an extracellular trophozoite stage (Hijjawi et al., 2002) (Rosales et al., 2005). This relationship and early divergence makes gregarines a crucial group in understanding apicomplexan evolution.

Within the Apicomplexa two species of extranuclear DNA have been observed. One resides within the apicoplast and another within the mitochondria. The apicoplast possesses a ~35-40 kb circular genome which has been sequenced in several apicomplexans including *Plasmodium falciparum* (Wilson et al., 1996), *Theileria parva* (Gardner et al., 2005), *Toxoplasma gondii,* and *Eimeria tenella* (Cai et al., 2004). The apicoplast genome contains genes for large and small subunit rRNAs, 25 species of tRNA, three subunits of a eubacterial RNA polymerase, 17 ribosomal proteins, and a translation elongation factor (Wilson et al., 1996) (Cai et al., 2004). The apicoplast has been found within a number of apicomplexans (Lang-Unnasch et al., 1998) however it is not present in *Cryptosporidium* (Zhu et al., 2000) (Abrahamsen et al., 2004) (Xu et al., 2004), and it also appears to be lacking in gregarines (Toso and Omoto, 2006).

Apicomplexans also possess extranuclear DNA within their mitochondria. The mitochondrial genome of *Plasmodium falciparum* is the smallest known mitochondrial

genome at 6kb, containing only three protein encoding genes (cytochrome oxidase III, cytochrome oxidase I and cytochrome b) and is a linear molecule (Feagin et al., 1991) (Feagin, 2000). The mitochondria genome has also been sequenced in *Theileria parva* and while it is 7.1 it also is linear and contains the same three genes as *Plasmodium falciparum* (Kairo et al., 1994) (Gardner et al., 2005). A candidate mitochondrial organelle in *Cryptosporidium* has been identified through studies of mitochondrial localized proteins (Riordan et al., 2003) (Slapeta and Keithly, 2004) (Putignani et al., 2004), however this organelle lacks a genome and none of the three genes found in the *Plasmodium* mitochondrial genome are present in the nuclear genome of *Cryptosporidium* (Abrahamsen et al., 2004) (Xu et al., 2004). Mitochondria have been observed with transmission electron microscopy in numerous gregarines (Reger, 1967) (Schrevel, 1971; Walsh and Callaway, 1969) (Desportes, 1974; Lucarotti, 2000); (Ciancio et al., 2001) (Landers, 2002) (Toso and Omoto, 2006), however, it is not known if the gregarine mitochondria contain their own genome.

All evidence suggests *Cryptosporidium* does not possess extranuclear DNA, either plastid or mitochondria. The postulated relationship between gregarines and *Cryptosporidium,* raises the question, "do gregarines possess extranuclear DNA?" We employed fluorescent microscopy and gel electrophoresis to seek out extranuclear DNA. PCR was utilized to amplify a mitochondrial gene, cytochrome oxidase subunit I (COXI) which has been found on every mitochondrial genome sequenced (Adams and Palmer, 2003), and Southern blot analysis was used to determine if this gene is extranuclear. We then applied a cloning strategy with Southern hybridizations to identify extranuclear DNA sequences.

MATERIALS AND METHODS

**Microscopy.** *Gregarina niphandrodes* trophozoites were dissected from *Tenebrio molitor* intestines in insect Ringer's (120 mM NaCl, 1.2 mM KCl, 1.4 mM $CaCl_2$) and fixed in –20°C methanol for 20 minutes. The trophozoites were washed in 100% ethanol 3 times prior to embedding in LR white resin. 1.5μm sections were cut on a Lecia Reichert microtome, and mounted on gelatin-coated slides.

A drop of 4'-6-diamidino-2-phenylindole (DAPI) (300nM in 0.05M Tris-HCl pH 7.2) was placed over the sections and incubated in the dark for 2 hr. Each slide was rinsed with distilled water and allowed to air dry. The slides were view on an Olympus BX60 microscope and photographed with a Nikon Coolpix 4500 digital camera.

**Collection of gametocysts from *G. niphandrodes***. Briefly, gametocysts from *G. niphandrodes* were collected from the frass of adult *Tenebrio molitor*, separated on a step sucrose gradient, manually collected, extensively washed in sterile distilled water, and stored in 100% ethanol at –20°C (Omoto et al., 2004).

**Extraction of DNA from gametocysts of *G. niphandrodes*.** *Gregarina. niphandrodes* gametocysts in 100% ethanol were rehydrated in sterile distilled water. The samples were frozen for 20 min at –80°C and incubated at 50°C for 15 min in lysis buffer (50 mM Tris-HCl, pH 8, 200 mM NaCl, 1 mM EDTA, pH 8, 1% (w/v) SDS, 0.2% (v/v) DTT). DNA was extracted using standard phenol-chloroform-isoamyl extraction and ethanol precipitation. The final pellet was suspended in sterile distilled water.

**Gel electrophoresis of total *G. niphandrodes* DNA.** *Gregarina niphandrodes* DNA was separated on 0.7% Tris-Acetate-EDTA (TAE) agarose gels with or without 0.6_g/ml ethidium bromide at 40V for 4 hr. The gel without ethidium bromide was post-

stained with Syber Gold (Invitrogen, Carlsbad, California). Both gels were viewed on a Dark Reader Transilluminator Model DR-45M (Clare Chemical Research, Dolores, CO) and photographed with a Nikon Coolpix 4500 digital camera.

**PCR**. Degenerate primers (CX1S1 and CX1AS1) Invitrogen (Carlsbad, CA) were used to amplify a segment of the COXI gene (Inagaki et al., 1997) using *G. niphandrodes* DNA as a template. Mg [4mM] and an annealing temperature of 55$^{o}$C was used. Products were separated on 1% agarose TAE agarose gel and visualized using Sybr Green (Invitrogen, Carlsbad, California) on the Dark Reader Transilluminator Model DR-45M.

**Phylogenetic analysis.** COXI sequences were aligned using ClustalX 1.83.1 and manually edited. Phylogenetic analysis was performed using PAUP 4.0b10. The tree was created using maximum-likelihood with the heuristic search option 1000 replicates. Sequences used for comparison were obtained from the following Apicoplexan species(GI#): *Plasmodium falciparum* (108744212), *Eimeria tenella* (32159197),*Theileria parva* (437862), *Toxoplasma gondii* (2897835). Insect species: *Tenebrio molitor* (27528773), *Simulium brevipar* (32364639), *Taygetis celia* (55420584), *Ithomia lagusa* (57790708). Alga species: *Volvox sp* (1731727). Haptophyte: *Isochrysis galbana* (2897781) and Viridiplantae: *Tetraedoron bitridens* (1731719).

**Cloning.** Total *G. niphandrodes* DNA was electrophoresed though a 0.7% TAE agarose gel with 0.6_g/ml ethidium bromide. The ~15 kb band was excised with a clean razor blade and the DNA extracted using the QIAEX II Gel Extraction Kit (Qiagen Valencia, CA). The DNA was concentrated using ethanol precipitation and digested with HindIII (Fermentas Hanover, MD) for 2 hr at 37$^{o}$C, ligated into pGEM-3Z vector

(Promega Madison, WI) and transformed into RapidTrans Competent & Extra Competent *E. coli* cells (Active Motif Carlsbad, Ca) according to manufacturers instructions.

**Sequencing.** Sequencing was done by the DyeDeoxy terminator cycle protocol with M13 primers for the cloned sequences and CX1S1 and CX1AS1 primers for the COXI PCR product. Sequencing reactions were analyzed on an Applied Biosystems 377 DNA Sequencer at the Washington State University Laboratory of Bioanalysis and Biotechnology.

**Southern Blot Analysis.** Hybridizations were performed according to the manufacturer's directions (Boehringer Mannheim DIG System Users Guide). *G. niphandrodes* DNA was electrophoresed through a 0.7% TAE agarose gel with 0.6_g/ml ethidium bromide. The DNA was depurinated with 250 mM HCl for 10 minutes followed by one water rinse. The DNA was denatured with 0.5N NaOH, 1.5M NaCl for 2x15min followed by a neutralization 2x15min of 0.5M Tris-HCl, 3M NaCl pH 7.0. The DNA was transferred to a Nytran Plus nylon membrane (Boehringer Mannheim) by standard capillary transfer overnight with 20X SSC and cross-linked to the membrane using Bio-Rad GS Gene Linker (Hercules, CA). The probes used were the COXI PCR product and sequences derived from cloning labeled with digoxigenin (DIG) using the PCR DIG Probe Synthesis Kit (Roche Diagnostics, Basel, Switzerland). Probes were denatured by boiling for 10 min followed by icing. The membrane was pre-hybridized with DIG Easy Hyb buffer (Roche Diagnostics) at 42°C for 2 h. Hybridization was performed overnight at 42°C with the DIG-labeled probes in Easy Hyb buffer. Membranes were washed 2 times for 15min with 2X SSX 0.1% SDS at room temperature and 2 times for 15min with 0.5X SSC 0.1% SDS at 68$^{o}$C. The probe was detected using anti-DIG-AP conjugate

(Roche Diagnostics) and the luminescence signal was imaged using an AutoBiochemi system (UVP, Upland, CA).

RESULTS

**Gregarines possess extranuclear DNA.** Staining with DAPI, a DNA specific fluorescent stain, demonstrated numerous punctate signals scattered throughout the cytoplasm as well as a strong nuclear signal in *G. niphandrodes* trophozoites (Fig. 1). This staining indicates the presence of extranuclear DNA.

Total *G. niphandrodes* DNA was electrophoresed through two different agarose gels, one with ethidium bromide and one without (Fig. 2). An extranuclear band is visible in the gel with ethidium bromide (Lane B). This band migrated slightly slower than the 12kb band in the 1kb ladder (Lane L). An extranuclear band is not evident in the gel without ethidium bromide, suggesting that the faster migration is due to differences in migration behavior of the band with the intercalating dye, ethidium bromide.

**Is the extranuclear DNA mitochondrial?** To investigate if this extranuclear DNA band was mitochondrial, we sought out a sequence commonly found on the mitochondrial genome of the Apicomplexa. The COXI gene is an ideal candidate since it is found in all mitochondria genomes (Adams and Palmer, 2003). Degenerate primers CX1S1 and CX1AS1 (Inagaki et al., 1997) were used to amplify a 377bp fragment of this gene (Fig. 3). This band was sequenced and revealed to be COXI. Phylogenetic analysis of this sequenced fragment is shown in Fig. 4. Our COXI sequence is monophyletic with other apicomplexan COXI genes and it clearly does not group with the host, *T. molitor* COXI sequence.

Next we performed a Southern blot analysis to determine if the COXI sequence localized to the extranuclear band (Fig. 5). The COX1 probe did not hybridize to the extranuclear band, but instead to the nuclear band (Fig. 5). This indicates that this COX1 sequence is localized on the nuclear genome rather than on the extranuclear band in *G. niphandrodes*.

**What is the nature of the extranuclear DNA?** In order to determine the sequence, and thus the nature of the extranuclear DNA, it was excised from the gel, restriction enzyme digested with HindIII, cloned and sequenced (Table 1). The great majority of clones, 32, did not form contigs with any other clone. These sequences also did not have any significant matches to sequences in the NCBI database by either BLASTN or BLASTX. The majority of the cloned sequences which formed contigs were rRNA genes, both large and small subunits. The rRNA genes formed a large contig of ~6.5kb which circularized (Fig. 6). To determine if these sequences were on the extranuclear band, a southern hybridization was performed using internal transcribed spacer region (ITS), between the large and small rRNA subunits, as a probe (Fig. 7). There was no hybridization to the extranuclear band with this probe. Thus despite the fact that these sequences constituted a large number of clones, it suggests that our procedure included significant ribosomal gene contamination, and indicates that the extranuclear DNA does not contain rRNA sequences.

To determine whether other clones originated from the extranuclear DNA, we tested probes from all clones which were represented by at least 2 clones (Table I). The probe of the contig formed by 3 clones (818bp long) hybridized to the extranuclear band

and not to the nuclear band (Fig. 7). The three other probes hybridized only to the nuclear band (data not show).

## DISCUSSION

To determine if gregarines possess extranuclear DNA we employed fluorescent microscopy and gel electrophoresis. PCR and Southern hybridizations were used to determine if the extranuclear band was mitochondrial. Also, a cloning strategy along with Southern hybridizations were used to begin to characterize this DNA.

Fluorescent microscopy revealed punctate extranuclear signals scattered throughout the *G. niphandrodes* trophozoite cytoplasm (Fig. 1). Using agarose gel electrophoresis we identified DNA unassociated with chromosomal DNA (Fig. 2). This piece of DNA migrates at a rate slightly slower than the 12kb linear marker. An extranuclear band is only visible in the gel stained with ethidium bromide and not Sybr Gold. This migration pattern suggests a circular structure in the extranuclear DNA band. Since ethidium bromide intercalates in supercoiled DNA less than linear DNA, closed circular DNA would migrate faster than linear DNA. This faster migration of the extranuclear DNA did not occur in the gel without ethidium bromide, therefore the extranuclear DNA was not resolved from the nuclear DNA. This variable migration indicates the band may be circular in nature.

This nonlinear migration was the first indication that this extranuclear DNA was different from all other extranuclear DNA studied in apicomplexans to date. The small size was significantly smaller than any plastid genome studied, and other evidence indicates that gregarines do not possess a plastid (Toso and Omoto, 2006). Also every apicomplexan mitochondrial genome studied to date is linear and 6-7kb. This

extranuclear band has more characteristics of a circular band and appears to be ~15kb, more that 2 times the size of apicomplexan mitochondrial genomes.

We identified a gene in gregarines that has been found in every other mitochondrial genome studied, COXI (Adams and Palmer, 2003) (Fig. 3). *G. niphanddrodes* has this gene, however, Southern blot analysis demonstrates that this gene does not reside on the extranuclear DNA but on the nuclear genome (Fig. 5). This finding indicates that the COXI, a mitochondrial gene, resides in the nuclear genome of gregarines, suggesting that gregarines may lack a mitochondrial genome. Thus gregarines are similar to *Cryptosporidium*, in that both possess mitochondria evident in transmission electron micrographs genome (Reger, 1967) (Walsh and Callaway, 1969) (Schrevel, 1971); (Desportes, 1974; Lucarotti, 2000) (Ciancio et al., 2001) (Landers, 2002) (Toso and Omoto, 2006) but lack a mitochondrial. However, in contrast, *Cryptosporidium* lacks COXI, a common mitochondrial enzyme, but *G. niphandrodes* has this gene. Our study does not indicate whether this gene is active in *G. niphandrodes*.

The hybridization of the COXI sequence to the nuclear DNA and not the extranuclear DNA supports the evidence in the gel electrophoresis study. This extranuclear DNA does not appear to be mitochondrial. It lacks the migration pattern of a linear mitochondrial genome, it is larger than all other known apicomplexan mitochondrial genomes and a gene, COXI that has been found on ever other mitochondrial genome studied is not present on this extranuclear DNA.

In our attempt to clone this extranuclear DNA, the majority of identified sequences were rRNA. 6.5kb of both large and small rRNA subunits formed contigs and circularized (Fig. 6). Yet, in Southern hybridization the probe designed from these

sequences did not hybridize to the extranuclear band, thus we must have had significant ribosomal RNA gene contamination. Further the extranuclear DNA does not contain rRNA genes (Fig. 7).

The circularization of the rRNA genes suggests two possibilities. The genes may form an episomal circle with tandem repeats. The genes must be repetitive or else the rRNA probes would have hybridized to a 6.5kb band, but instead it hybridized to the high molecular weight DNA in the gel. Also a band of 6.5kb is not visible on gel electrophoresis of total *G. niphandrodes* DNA. The second possibility is that the rRNA gene cluster is highly repetitive. In such a case, we would expect the clones to circularize. Ribosomal RNA gene cluster is not found in highly repetitive tandem repeats in any other published apicomplexan genomes. For example, *C. parvum* and *C. hominis* have only five copies of the 5.8*S*, 18*S*, and 28*S* rRNA units (Abrahamsen et al., 2004) (Xu et al., 2004), *P. falciparum* has seven copies (Gardner et al., 2002) and *Theileria parva* has two copies (Gardner et al., 2005). These are all found in separate locations on the genome, and not as tandem repeats. *G. niphandrodes* may possess many more copies, and in tandem repeats.

Only one clone (818 bp) hybridized to the extranuclear band (Fig. 7) It's closest match using BLASTX is Zn-finger, CCHC type and RNA-directed DNA polymerase and integrase, catalytic domain containing protein ($e=3e^{-19}$) (Table 1). The sequence does not appear to be mitochondrial, since neither BLASTN, BLASTX, or TBLASTX reveals any mitochondrial sequences against the NCBI database. Due to the relationship between gregarines and *Cryptosporidium* similar BLAST searches were performed using the *Cryptosporidium* database (http://cryptodb.org/cryptodb/). There were no significant

matches. At present time the nature of this extranuclear DNA is still unknown, however it is not likely to be plastid or mitochondrial.

ACKNOWLEDGEMENTS

We thank the WSU Franceschi Microscopy and Imaging Center, namely Chris Davitt, Valerie Lynch-Holm, and the late Vince Franceschi for assistance and guidance in microcopy. Eric Roalson for help and insight. Don Knowles and Lowell Kappmeyer for *B. equis* DNA and technical assistance. Michelle Martin, Kyle Martin, and Kelly Ramerizfor gametocysts collection. Derek Pouchnik, WSU Laboratory for Bioanalysis and Biotechnology, for DNA sequencing. Dr. John Janovy, University of Nebraska, Lincoln, for instruction with *T. molitor* and gregarine care. John Dahl and Eric Shelden for technical assistance. Andris Kleinhofs for advise.

Literature Cited

Abrahamsen, M., Templeton, T., Enomoto, S., Abrahante, J., Zhu, G., Lancto, C., Deng, M., Liu, C., Widmer, G., Tzipori, S., Buck, G., Xu, P., Bankier, A., Dear, P., Konfortov, B., Spriggs, H., Iyer, L., Anantharaman, V., Aravind, L. and Kapur, V. 2004. Complete genome sequence of the apicomplexan, *Cryptosporidium parvum*. Science, **304**: 441-445.

Adams, K. and Palmer, J. 2003. Evolution of mitochondrial gene content: gene loss and transfer to the nucleus. Mol. Phylogenet. Evol., **29**: 380-395.

Cai, X., Fuller, A., McDougald, L. and Zhu, G. 2004. Apicoplast genome of the coccidian *Eimeria tenella*. Gene, **321**: 39-46.

Carreno, R., Martin, D. and Barta, J. 1999. *Cryptosporidium* is more closely related to the gregarines than to coccidia as shown by phylogenetic analysis of apicomplexan

parasites inferred using small-subunit ribosomal RNA gene sequences. Parasitol. Res., **85**: 899-904.

Ciancio, A., Scippa, S. and Cammarano, M. 2001. Ultrastructure of trophozoites of the gregarine *Lankesteria ascidiae* (Apicomplexa : Eugregarinida) parasitic in the ascidian *Ciona intestinalis* (Protochordata). Eur. J. Protistol., **37**: 327-336.

Desportes, I. 1974. Ultrastructure et Evolution Nucleaire des Trophozoites d'une Gregarine d'Ephemeroptere: *Enterocystis fungoides* M. Codreanu. J Protozool, **21**: 83-94.

Feagin, J. 2000. Mitochondrial genome diversity in parasites. Int J Parasitol, **30**: 371-390.

Feagin, J., Gardner, M., Williamson, D. and Wilson, R. 1991. The putative mitochondrial genome of *Plasmodium falciparum*. Journal of Protozoology, **38**: 243-245.

Gardner, M., Bishop, R., Shah, T., de Villiers, E., Carlton, J., Hall, N., Ren, Q., Paulsen , I., Pain, A., Berriman, M., Wilson, R., Sato, S., Ralph, S., Mann, D., Xiong, Z., Shallom, S., Weidman , J., Jiang, L., Lynn, J., Weaver, B., Shoaibi, A., Domingo, A., Wasawo, D., Crabtree, J., Wortman, J., Haas, B., Angiuoli, S., Creasy, T., Lu, C., Suh, B., Silva, J., Utterback, T., Feldblyum, T., Pertea, M., Allen, J., Nierman, W., Taracha, E., Salzberg, S., White, O., Fitzhugh, H., Morzaria, S., Venter, J., Fraser, C. and Nene, V. 2005. Genome sequence of *Theileria parva*, a bovine pathogen that transforms lymphocytes. Science, **309**: 134-137.

Gardner, M., Hall, N., Fung, E., White, O., Berriman, M., Hyman, R., Carlton, J., Pain, A., Nelson, K., Bowman, S., Paulsen, I., James, K., Eisen, J., Rutherford, K., Salzberg, S., Craig, A., Kyes, S., Chan, M., Nene, V., Shallom, S., Suh, B., Peterson, J., Angiuoli, S., Pertea, M., Allen, J., Selengut, J., Haft , D., Mather, M.,

Vaidya, A., Martin, D., Fairlamb, A., Fraunholz, M., Roos, D., Ralph, S., McFadden, G., Cummings, L., Subramanian, G., Mungall, C., Venter, J., Carucci, D., Hoffman, S., Newbold, C., Davis, R., Fraser, C. and Barrell, B. 2002. Genome sequence of the human malaria parasite *Plasmodium falciparum*. Nature, **3**: 498-511.

Hijjawi, N., Meloni, B., Ryan, U., Olson, M. and Tamavo, S. 2002. Successful *in vitro* cultivation of *Cryptosporidium andersoni*: evidence for the existence of novel extracellular stages in the life cycle and implications for the classification of *Cryptosporidium*. Internat. J. Parasitol., **32**: 1719-1726.

Inagaki, Y., Hayashi-Ishimaru, Y., Ehara, M., Igarashi, I. and Ohama, T. 1997. Algae or protozoa: phylogenetic position of euglenophytes and dinoflagellates as inferred from mitochondrial sequences. J. Mol. Evol., **45**: 295-300.

Kairo, A., Fairlamb, A., Gobright, E. and Nene, V. 1994. A 7.1 kb linear DNA molecule of *Theileria parva* has scrambled rDNA sequences and open reading frames for mitochondrially encoded proteins. EMBO J., **13**: 898-905.

Kohler, S., Delwiche, C., Denny, P., Tilney, L., Webster, P., Wilson, R., Palmer, J. and Roos, D. 1997. A plastid of probable green algal origin in apicomplexan parasites. Science, **275**: 1485-1489.

Landers, S. 2002. The fine structure of the gamont of *Pterospora floridiensis* (Apicomplexa: Eugregarinida). J Eukaryot Microbiol, **49**: 220-226.

Lang-Unnasch, N., Reith, M., Munholland, J. and Barta, J. 1998. Plastids are widespread and ancient in parasites of the phylum Apicomplexa. Internat. J. Parasitol., **28**: 1743-1754.

Leander, B., Clopton, R. and Keeling, P. 2003. Phylogeny of gregarines (Apicomplexa) as inferred from small-subunit rDNA and beta-tubulin. Int. J. Syst. Evol. Microbiol., **53**: 345-354.

Lucarotti, C. 2000. Cytology of *Leidyana canadensis* (Apicomplexa : Eugregarinida) in *Lambdina fiscellaria fiscellaria* larvae (Lepidoptera : Geometridae). J Invertebr Pathol, **75**: 117-125.

McFadden, G. and van Dooren, G. 2004. Evolution: red algal genome affirms a common origin of all plastids. Curr Biol, **14**: R514-516.

Omoto, C., Toso, M., Tang, K. and Sibley, L. 2004. Expressed sequence tag (EST) analysis of gregarine gametocyst development. Int J Paraitol, **34**: 1261-1271.

Putignani, L., Tait, A., Smith, H.V., Horner, D., Tovar, J., Tetley, L. and Wastling, J.M. 2004. Characterization of a mitochondrion-like organelle in *Cryptosporidium parvum*. Parasitiol, **129**: 1-18.

Reger, J. 1967. The fine structure of the gregarine *Pyxinoides balani* parasitic in the barnacle *Balanus tintinnabulum*. J Protozool, **14**: 488-497.

Riordan, C., Ault, J., Langreth, S. and Keithly, J. 2003. *Cryptosporidium parvum* Cpn60 targets a relict organelle. Curr. Genet., **44**: 138-147.

Rosales, M., Cordon, G., Moreno, M., Sanchez, C. and Mascaro, C. 2005. Extracellular like-gregarine stages of *Cryptosporidium parvum*. Acta Trop, **95**: 74-78.

Schrevel, J. 1971. Observations Biologiques et Ultrastructure sur les *Selenidiida* et Leurs Consequences sur la Systematique des *Gregarinomorphes*. Journal of Protozoology, **18**: 448-470.

Slapeta, J. and Keithly, J. 2004. *Cryptosporidium parvum* mitochondrial-type HSP70 targets homologous and heterologous mitochondria. Eukaryot Cell, **3**: 483-494.

Toso, M. and Omoto, C. 2006. *Gregarina niphandrodes* Lacks Both a Plastid Genome and Organelle. J. Eukaryot. Microbiol., In Press.

Walsh, R.J. and Callaway, C. 1969. The fine structure of the gregarine *Lankesteria culicis* parasitic in the yellow fever mosquito *Aedes aegypti*. J Protozool, **16**: 536-545.

Wilson, R., Denny, P., Preiser, P., Rangachar, K., Roberts, K., Roy, A., Whyte, A., Strath, M., Moore, D., Moore, P. and Williamson, D. 1996. Complete gene map of the plastid-like DNA of the malaria parasite *Plasmodium falciparum*. J Mol Biol, **216**: 155-172.

Xu, P., Widmer, G., Wang, Y., Ozaki, L., Alves, J., Serrano, M., Puiu, D., Manque, P., Akiyoshi, D., Mackey, A., Pearson, W., Dear, P., Bankier, A., Peterson, D., Abrahamsen, M., Kapur, V., Tzipori, S. and Buck, G. 2004. The genome of *Cryptosporidium hominis*. Nature, **431**: 1107-1112.

Zhu, G., Marchewka, M. and Keithly, J. 2000. *Cryptosporidium parvum* appears to lack a plastid genome. Microbiology, **146**: 315-321.

Table 1 Cloning and Southern Results

| Number of Clones | BLASTN | BLASTX | Size of contig (bp) | Southern |
|---|---|---|---|---|
| 32 | ns | ns | no contigs formed with other clones | nd |
| 24 | rRNA genes | | 6500 | - |
| 2 | ns | ns | 411 | - |
| 2 | ns | ns | 1109 | - |
| 3 | ns | Zn-finger, CCHC type and RNA-directed DNA polymerase and Integrase, catalytic domain containing protein ($e=3e^{-19}$) | 818 | + |
| 2 | ns | ns | 188 | - |

ns – no significant match; nd- not done
(+) Probe hybridized to extranuclear band in Southern hybridization.
(-) Probe hybridized to nuclear band in Southern hybridization.

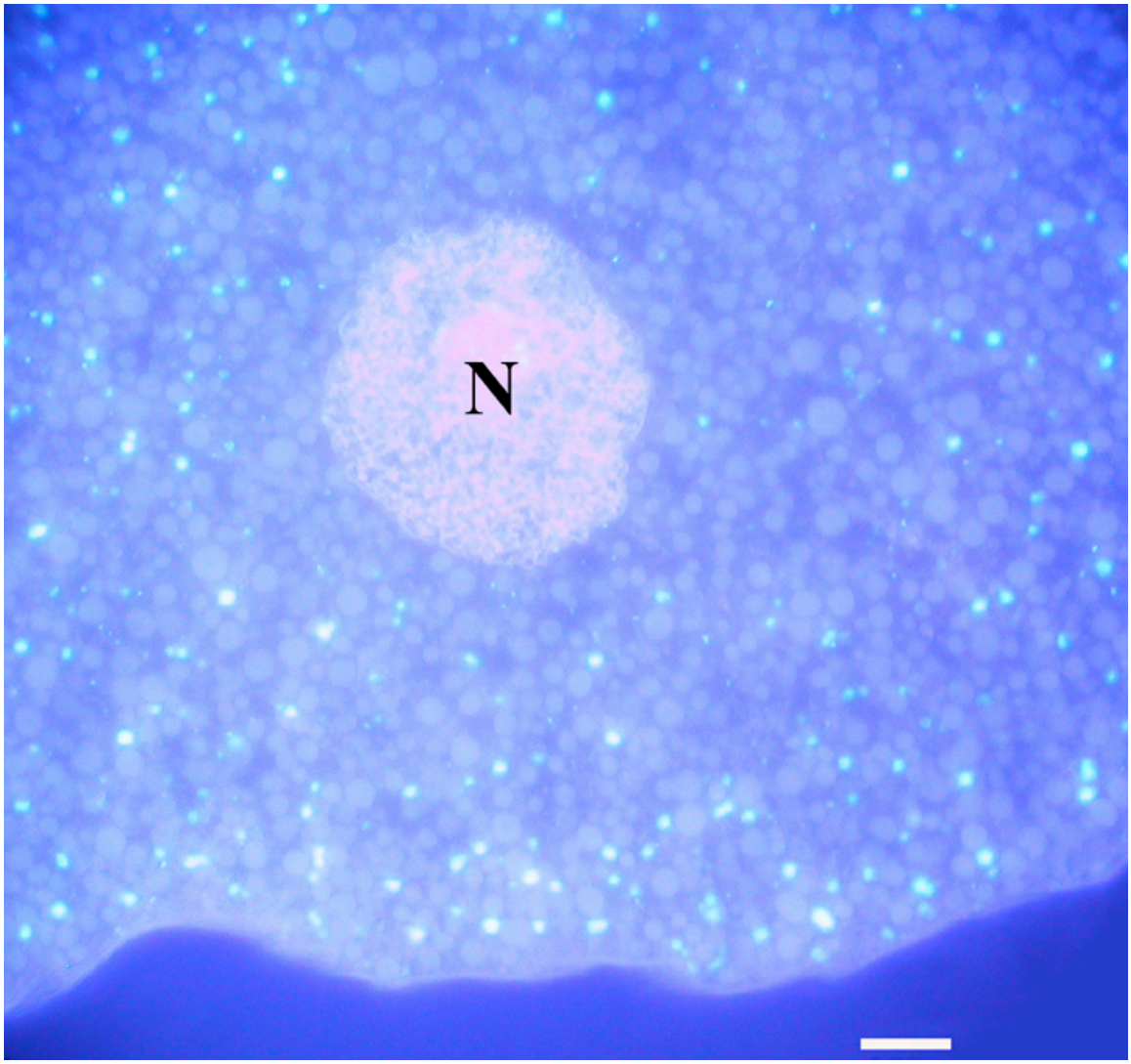


Figure **1**. DAPI staining of *G. niphandrodes* trophozoite. Nucleus (N) is brightly stained as are numerous extranuclear structures dispersed throughout the cytoplasm. Scale bar- 10_m

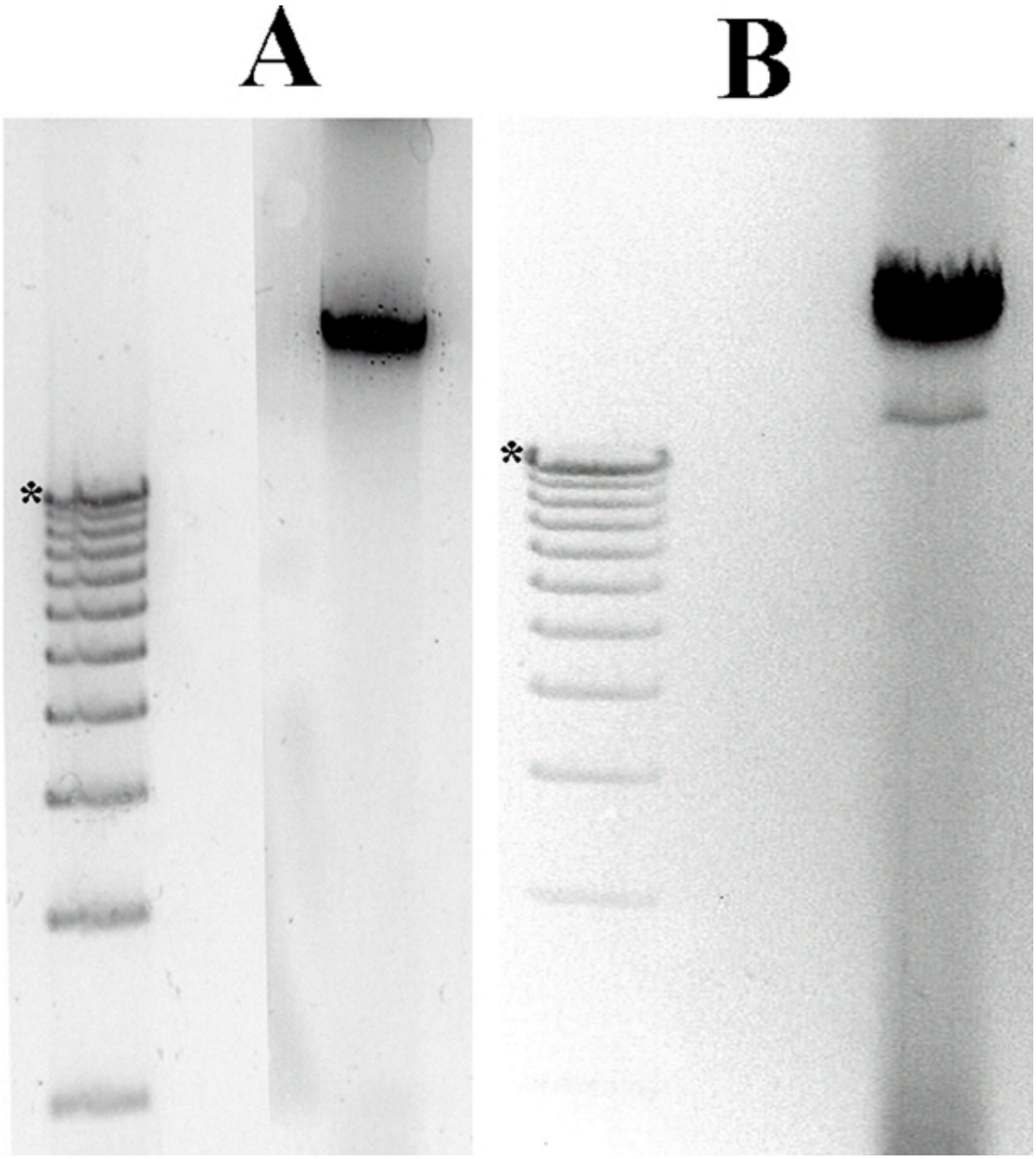


Figure **2**. Gel electrophoresis of total *G. niphandrodes* DNA. Lane L 1kb ladder Lane (A) gel without ethidium bromide poststained with Sybr Gold. Lane (B) gel with ethidium bromide. The heavy dark band of nuclear DNA is visible in both gels. A band which migrates slightly above the 12kb(*) band is visible in Lane B.

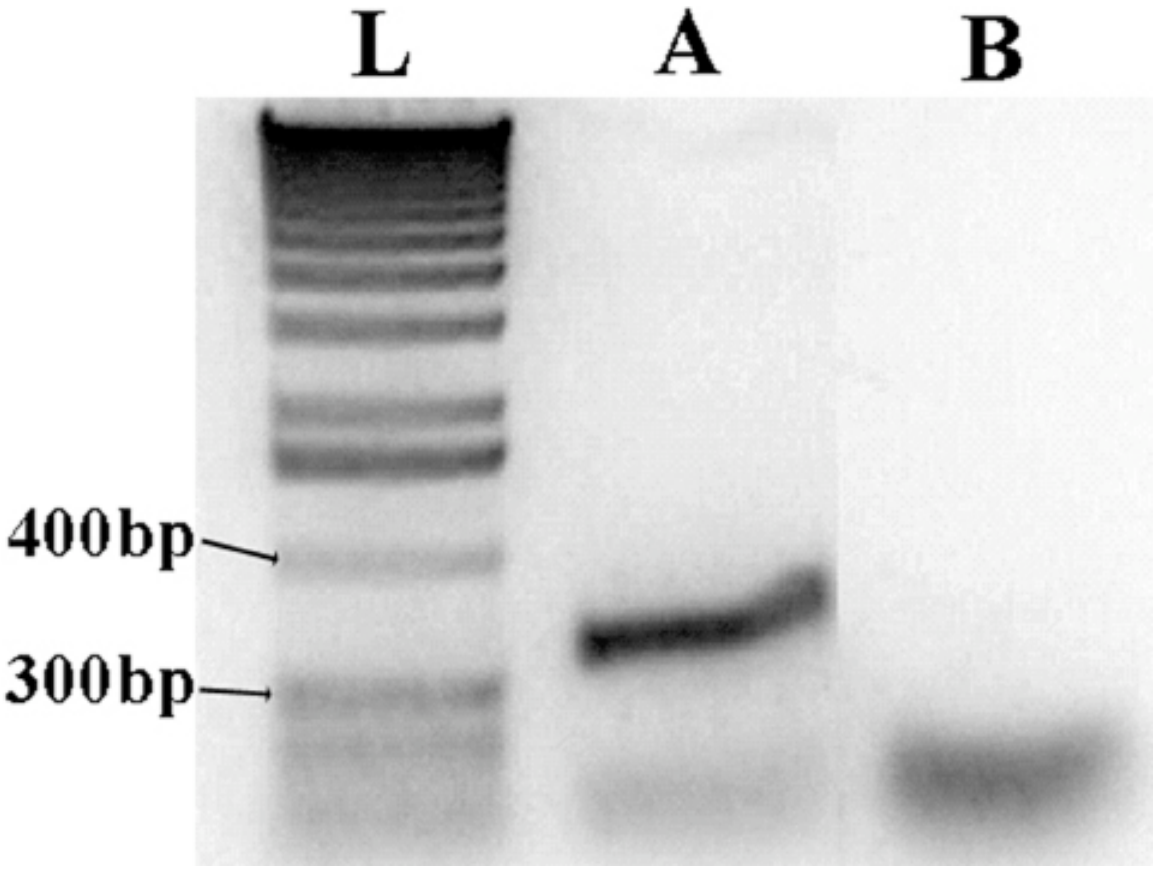


Figure **3.** Agarose gel of COX1 PCR products. A strong amplicon band is obtained using *G. niphandrodes* DNA as a template (Lane A). Negative control without *G. niphandrodes* (lane B) the primer band is visible at the bottom of the gel. Lane L, 100bp ladder.

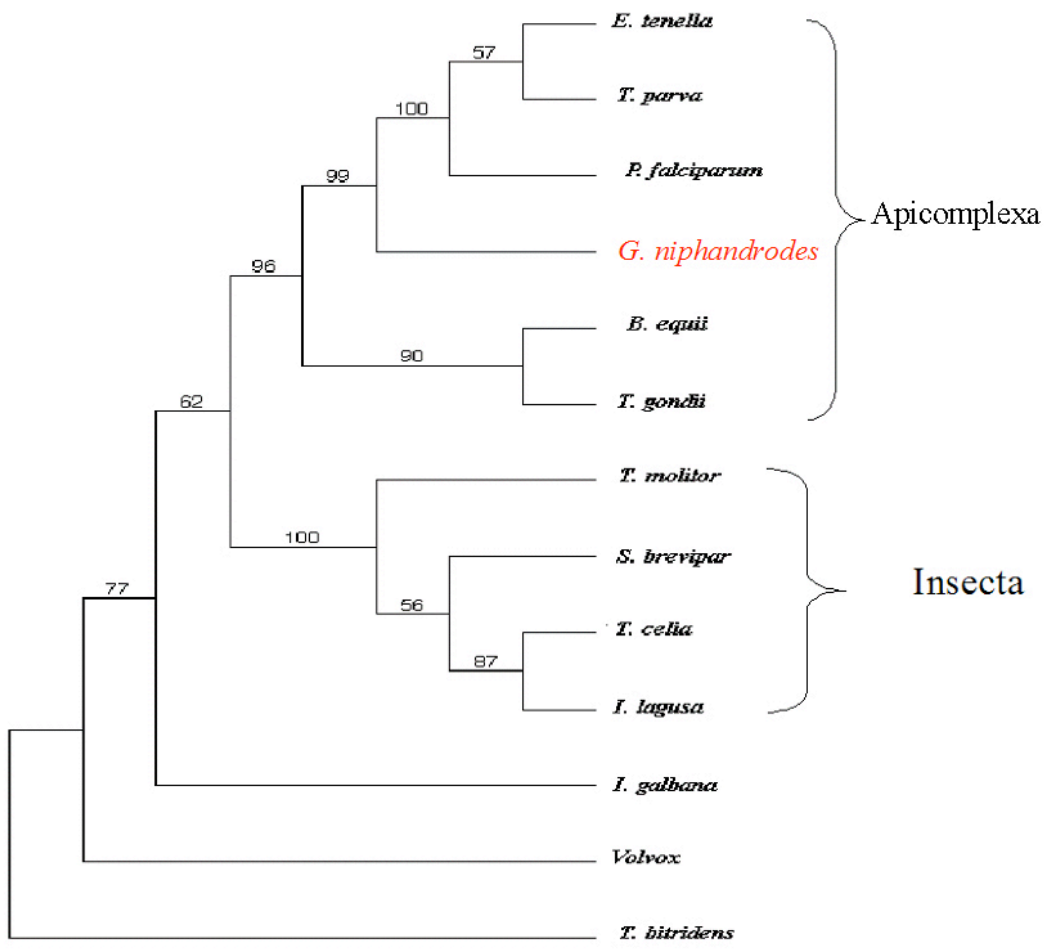


Figure **4.** A maximum-likelihood phylogenetic tree of the COX1 gene. *G. niphandrodes* COXI sequence is monophyletic with other apicomplexan COXI genes and groups with other protist COXI.

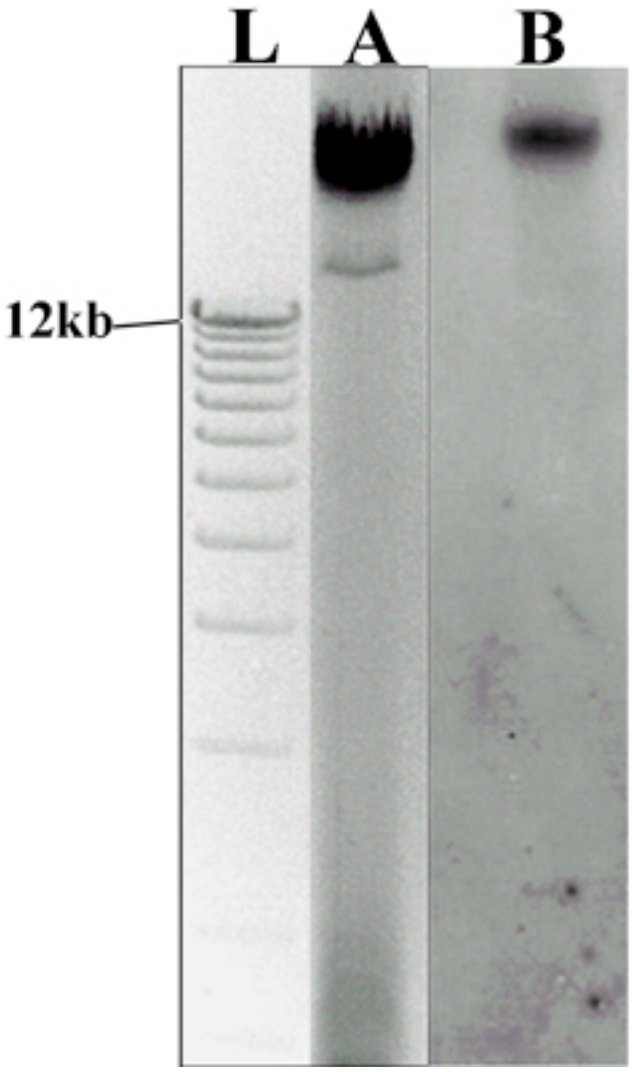


Figure **5**. Southern blot analysis of *G. niphandrodes* COXI gene. Agarose gel of total *G. niphandrodes* DNA (A) and 1kb ladder (L). Lane B is a southern blot of the gel in lane A using the *G. niphandrodes* COXI PCR product as a probe. The probe hybridized to the nuclear DNA and not the extranuclear band.

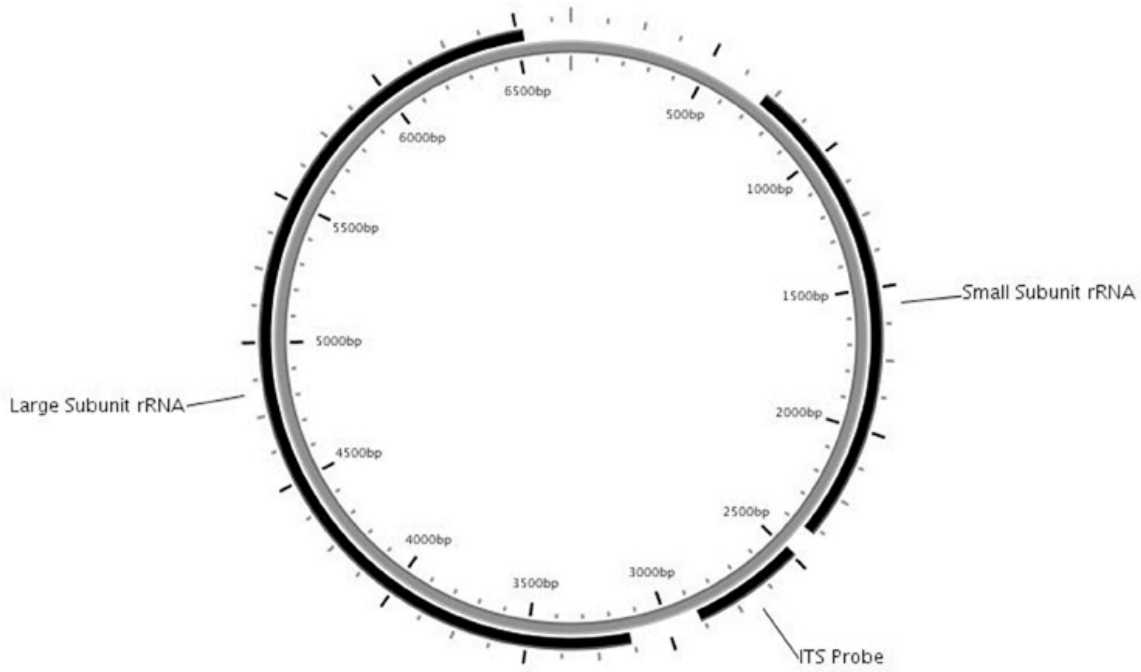


Figure **6.** A map of the large and small subunits of *G. niphandrodes*. The region used as probe in Southern analysis is noted.

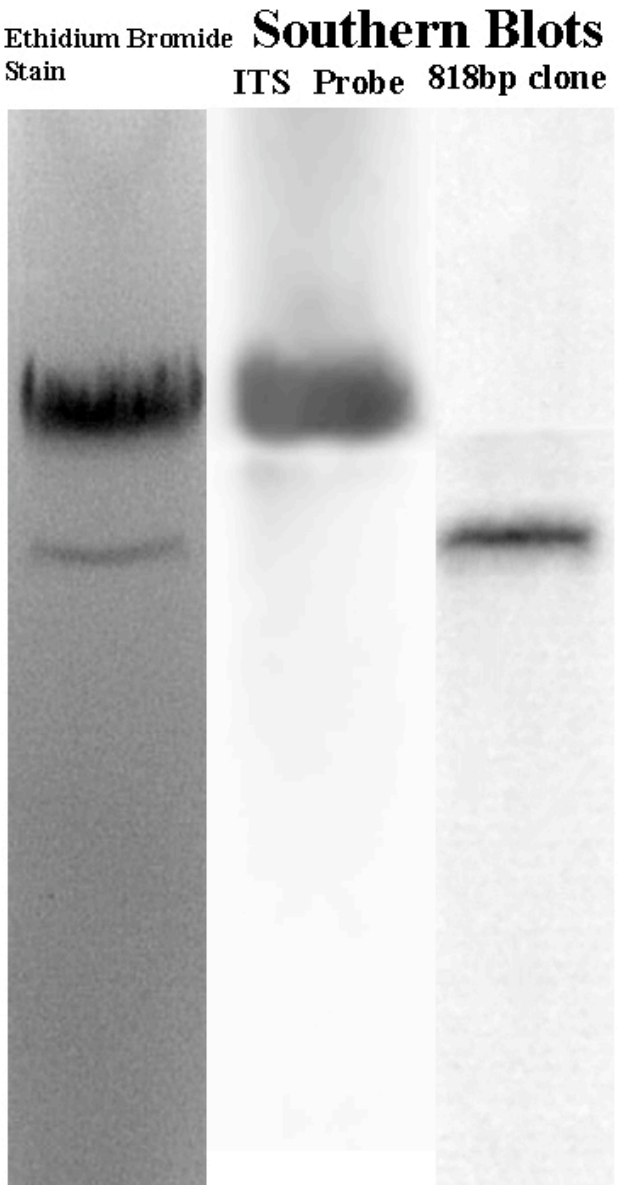


Figure **7.** Southern blot analysis. The left lane is total *G. niphandrodes* DNA on a 0.7% agarose gel. Center lane is a Southern hybridization of the ITS probe, which hybridized to the nuclear DNA and not the extranuclear DNA. Right lane is a Southern hybridization using a probe designed from the contig containing 818 bases which hybridized to the extranuclear band.

## GENERAL CONCLUSIONS

The phylum Apicomplexa presents a unique system for investigating evolution of endosymbiosis, and the reduction of organelle genomes. Many apicomplexans possess two organelles derived from endosymbiosis: the apicoplast and the mitochondria. Genomes associated with the two organelles are highly reduced compared to other plastid and mitochondrial genomes. *Cryptosporidium* is an extreme case in that it lacks both the plastid organelle/genome and the mitochondrial genome (Abrahamsen et al., 2004; Xu et al., 2004; Zhu et al., 2000). A sister relationship between gregarines and *Cryptosporidium* and their early divergence in the phylum has been suggested based upon phylogenetic studies of the small rRNA subunit (Carreno et al., 1999). This purported relationship raises questions regarding the status of endosymbiotic-derived organelles and their genomes in gregarines. We set out to determine if gregarines possessed a plastid and its genome and mitochondria and its genome.

We have demonstrated that *G. niphandrodes* lack an apicoplast and its corresponding genome through genomic studies utilizing PCR and Southern hybridizations along with inhibitor and electron microscopy studies (Toso and Omoto, 2006). Using PCR, Southern hybridizations and electron microscopy studies we also showed that gregarines appear to lack a mitochondrial genome yet retain a mitochondria-like organelle. Thus our data indicate that gregarines are more similar to *Cryptosporidium* in their status of extranuclear DNA in that they lack both plastid and mitochondrial genomes.

Phylogenetic analysis of glyceraldehyde-3-phosphate dehydrogenase gene suggests that apicomplexan plastids share a common ancestor with dinoflagellate and heterokont plastids (Fast et al., 2001) (Dick et al.) Genome analysis of *Cryptosporidium* revealed that several of its genes are cyanobacterial in origin (Huang et al., 2004) supporting the idea that an ancestor of *Cryptosporidium* harbored a plastid. The most parsimonious interpretation of this shared ancestry is that an ancestor of *Cryptosporidium* and gregarines harbored a plastid, but when the apicomplexan lineages diverged, the plastid along with it's corresponding genome was lost.

The situation with mitochondria is slightly different. Apicomplexans have the smallest know mitochondrial genome with only three protein-encoding genes (Feagin, 2000; Feagin et al., 1991). However, *Cryptosporidium* lacks the genome altogether (Abrahamsen et al., 2004; Xu et al., 2004; Zhu et al., 2000). Furthermore, none of the commonly found mitochondrial genome sequences are found in *Cryptosporidium's* nuclear genome. Yet *Cryptosporidium* possesses an organelle that appears similar to mitochondria (Putignani, 2005; Putignani et al., 2004; Slapeta and Keithly, 2004). Our study strongly suggests that gregarines appear to also lack a mitochondrial genome. However, a sequence found in every other mitochondrial genome sequenced, COXI gene, is present in *G. niphandrodes* but appears to reside in the nuclear genome. Thus gregarines, unlike *Cryptosporidium,* has retain in its nuclear genome some of the sequences normally found in the mitochondrial genome.

These "mitochondrial" organelles of *Cryptosporidium* and gregarines are similar to those of other amitochondrial protist such as Microsporidia (Peyretaillade et al., 1998) and *Entamoeba histolytica* (Clark and Roger, 1995). These species possess mitosomes

and hydrogenosomes (Regoes et al., 2005). Protein localization and phylogenetic studies have demonstrated that mitosomes and hydrogenosomes are related to mitochondria (Embley et al., 2003). Hydrogenosomes produce molecular hydrogen through fermentation, lack cytochromes, function in FeS cluster biosynthesis, and usually lack DNA (Martin, 2005). At present, the knowledge of mitosomes is very limited. A NCBI search (http://www.ncbi.nlm.nih.gov/) only reveals 13 articles on mitosomes. FeS cluster is the only known shared function among all of these mitochondria-like organelles. FeS cluster has also been noted as a function of *Cryptosporidium's* "mitochondrion" (Putignani et al., 2004). Future work on mitochondrial genes and functions of the gregarine mitochondria may provide interesting intermediates to the reduction of mitochondria.

## Literature Cited


Abrahamsen, M., Templeton, T., Enomoto, S., Abrahante, J., Zhu, G., Lancto, C., Deng, M., Liu, C., Widmer, G., Tzipori, S., Buck, G., Xu, P., Bankier, A., Dear, P., Konfortov, B., Spriggs, H., Iyer, L., Anantharaman, V., Aravind, L. and Kapur, V. 2004. Complete genome sequence of the apicomplexan, *Cryptosporidium parvum*. Science, **304**: 441-445.

Carreno, R., Martin, D. and Barta, J. 1999. *Cryptosporidium* is more closely related to the gregarines than to coccidia as shown by phylogenetic analysis of apicomplexan parasites inferred using small-subunit ribosomal RNA gene sequences. Parasitol. Res., **85**: 899-904.

Clark, C. and Roger, A. 1995. Direct evidence for secondary loss of mitochondria in Entamoeba histolytica. Proc Natl Acad Sci USA, **92**: 6518-6521.

Dick, S., van Poppel, N. and Vermeulen, A. 2001. Intron invasion in protozoal nuclear encoded plastid genes. Molecular and Biochemical Parasitology, **15**: 119-121.

Embley, T., van der Giezen , M., Horner, D., Dyal, P., Bell, S. and Foster, P. 2003. Hydrogenosomes, mitochondria and early eukaryotic evolution. IUBMB Life, **55**: 387-395.

Fast, N., Kissinger, J., Roos, D. and Keeling, P. 2001. Nuclear-encoded, plastid-targeted genes suggest a single common orgin for apicomplexan and dinoflagellate plastids. Mol. Biochem. Evol., **18**: 418-426.

Feagin, J. 2000. Mitochondrial genome diversity in parasites. Int J Parasitol, **30**: 371-390.

Feagin, J., Gardner, M., Williamson, D. and Wilson, R. 1991. The putative mitochondrial genome of *Plasmodium falciparum*. Journal of Protozoology, **38**: 243-245.

Huang, J., Mullapudi, N., Lancto, C., Scott, M., Abrahamsen, M. and Kissinger, J. 2004. Phylogenomic evidence supports past endosymbiosis, intracellular and horizontal gene transfer in *Cryptosporidium parvum*. Genome Biol, 11.

Martin, W. 2005. The missing link between hydrogenosomes and mitochondria. Trends. Microbiol., **13**: 257-259.

Peyretaillade, E., Broussolle, V., Peyret, P.M., G, Gouy, M. and Vivares, C. 1998. Microsporidia, amitochondrial protists, possess a 70-kDa heat shock protein gene of mitochondrial evolutionary origin. Mol Biol Evol, **15**: 683-689.

Putignani, L. 2005. The unusual architecture and predicted function of the mitochondrion organelle in *Cryptosporidium parvum* and *hominis* species: the strong paradigm of the structure-function relationship. Parasitologia, **47**: 217-225.

Putignani, L., Tait, A., Smith, H.V., Horner, D., Tovar, J., Tetley, L. and Wastling, J.M. 2004. Characterization of a mitochondrion-like organelle in *Cryptosporidium parvum*. Parasitiol, **129**: 1-18.

Regoes, A., Zourmpanou, D., Leon-Avila, G., van der Giezen, M., Tovar, J. and Heh, l.A. 2005. Protein import, replication and inheritance of a vestigial mitochondrion. J Biol Chem,

Slapeta, J. and Keithly, J. 2004. *Cryptosporidium parvum* mitochondrial-type HSP70 targets homologous and heterologous mitochondria. Eukaryot Cell, **3**: 483-494.

Toso, M. and Omoto, C. 2006. *Gregarina niphandrodes* Lacks Both a Plastid Genome and Organelle. J Eukaryot Microbiol, In Press.

Xu, P., Widmer, G., Wang, Y., Ozaki, L., Alves, J., Serrano, M., Puiu, D., Manque, P., Akiyoshi, D., Mackey, A., Pearson, W., Dear, P., Bankier, A., Peterson, D., Abrahamsen, M., Kapur, V., Tzipori, S. and Buck, G. 2004. The genome of *Cryptosporidium hominis*. Nature, **431**: 1107-1112.

Zhu, G., Marchewka, M. and Keithly, J. 2000. *Cryptosporidium parvum* appears to lack a plastid genome. Microbiology, **146**: 315-321.

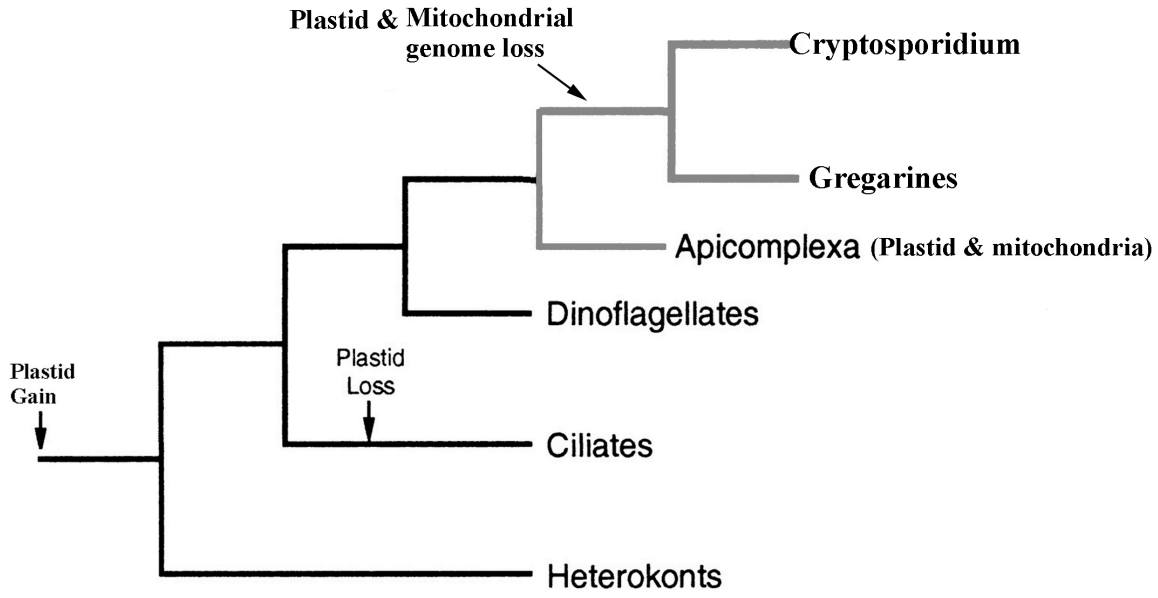


Figure 1. Diagram illustrating the proposed gains and losses of plastid organelle and genome and the mitochondrial genome (Adapted from Fast et al., 2001).